JOURNAL OF GEOPHYSICAL RESEARCH, VOL. 96, NO. C8, PAGES 14,743–14,768, AUGUST 15, 1991

The Nature of the Cold Filaments in the California Current System

P. TED STRUB, P. MICHAEL KOSRO, AND ADRIANA HUYER

College of Oceanography, Oregon State University, Corvallis

CTZ COLLABORATORS[1]

Data from the Coastal Transition Zone (CTZ) experiment are used to describe the velocity fields and water properties associated with cold filaments in the California Current. Combined with previous field surveys and satellite imagery, these show seasonal variability with maximum dynamic height ranges and velocities in summer and minimum values in late winter and early spring. North of Point Arena (between 39°N and 42°N) in spring–summer the flow field on the outer edge of the cold water has the character of a meandering jet, carrying fresh, nutrient-poor water from farther north on its offshore side and cold, salty, nutrient-rich water on its inshore side. At Point Arena in midsummer, the jet often flows offshore and continues south without meandering back onshore as strongly as it does farther north. The flow field south of Point Arena in summer takes on more of the character of a field of mesoscale eddies, although the meandering jet from the north continues to be identifiable. The conceptual model for the May–July period between 36°N and 42°N is thus of a surface jet that meanders through and interacts with a field of eddies; the eddies are more dominant south of 39°N, where the jet broadens and where multiple jets and filaments are often present. At the surface, the jet often separates biological communities and may appear as a barrier to cross-jet transport, especially north of Point Arena early in the season (March–May). However, phytoplankton pigment and nutrients are carried on the inshore flank of the jet, and pigment maxima are sometimes found in the core of the jet. The biological effect of the jet is to define a convoluted, 100 to 400-km-wide region next to the coast, within which much of the richer water is contained, and also to carry some of that richer water offshore in meanders along the outer edge of that region.

1. INTRODUCTION AND BACKGROUND

Several different velocity structures have been hypothesized to be associated with the cold filaments seen in satellite imagery from the California Current system and other eastern boundary currents [*Bernstein et al.*, 1977; *Traganza et al.*, 1983; *Flament et al.*, 1985; *Kelly*, 1985; *Shannon et al.*, 1985; *Johannessen et al.*, 1989]. The purpose of this paper is to summarize the evidence from the Coastal Transition Zone (CTZ) experiment and previous field studies with respect to the hypothesized velocity structures. The questions addressed are, (1) What is the spatial structure of the velocities and water properties associated with the filaments? (2) What is the temporal variability of that structure? (3) What are the biological implications of that structure and variability?

Three simplified conceptual models of the filaments are shown in Figure 1. "Squirts" are one-way jets, transporting coastally upwelled water to the deep ocean, perhaps terminating in a counterrotating vortex pair, with a shape in the sea surface temperature (SST) and pigment fields often referred to as "mushroom," "hammerhead," or "T" [*Ikeda and Emery*, 1984; *Davis*, 1985]. Onshore flow may occur in a broader and weaker return flow between the offshore squirts and/or in subsurface flow. The idealized squirt is generated by nearshore convergences, such as caused by local wind relaxations around capes [*Huyer and Kosro*, 1987; *Send et al.*, 1987] or other mechanisms [*Stern*, 1986]. The biological implication of this structure is that a large amount of enriched, salty, and cold coastally upwelled water (and biomass) is transported to the deep ocean.

An alternate conceptual model consists of a number of mesoscale eddies imbedded in a slow southward current [*Mooers and Robinson*, 1984; *Rienecker et al.*, 1987]. Where the eddies draw recently upwelled water away from the coast, they create a surface temperature structure similar to a squirt. The difference is that the pure squirt model envisions the generation by convergences in the nearshore region and the mesoscale eddy model envisions the offshore eddy field as the source of energy. The implication for nutrients and biomass is that offshore transport over long time periods should be accomplished by large-scale "eddy diffusion," i.e., quasi-random motions of parcels exchanged between eddies, parameterized by an eddy diffusivity that may vary with location and direction (alongshore versus offshore).

The third conceptual model consists of a continuous southward jet, meandering offshore and onshore. During

[1]C. James, L. J. Walstad, R. L. Smith, J. A. Barth, R. R. Hood, and M. R. Abbott, College of Oceanography, Oregon State University, Corvallis; K. H. Brink, Woods Hole Oceanographic Institution, Woods Hole, Massachusetts; T. L. Hayward, P. P. Niiler, and M. S. Swenson, Scripps Institution of Oceanography, La Jolla, California; R. K. Dewey, Science Applications International Corporation, Bellevue, Washington; F. Chavez, Monterey Bay Aquarium Research Institute, Pacific Grove, California; S. R. Ramp, M. L. Batteen, and R. L. Haney, Naval Postgraduate School, Monterey, California; D. L. Mackas, Institute of Ocean Sciences, Sidney, British Columbia; L. Washburn, University of California, Santa Barbara; D. C. Kadko, University of Miami, Miami, Florida; R. T. Barber, Duke University, Marine Laboratory, Beaufort, North Carolina; D. B. Haidvogel, Institute of Marine and Coastal Sciences, Rutgers University, New Brunswick, New Jersey.

Page number 91JC01024.
0148-0227/91/91JC-01024$05.00

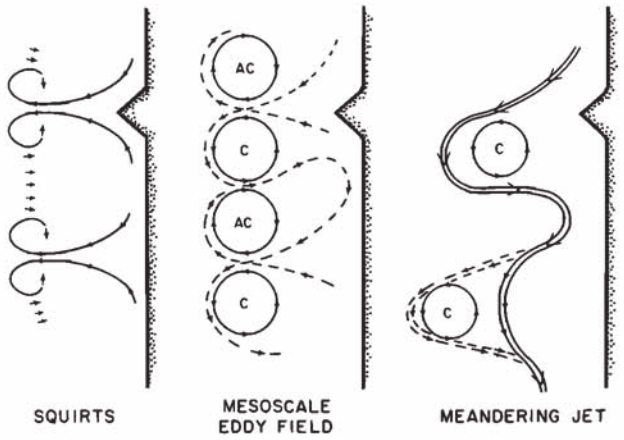

Fig. 1. The three simple conceptual models considered for the flow structure associated with the cold filaments.

its onshore excursions, it may entrain coastally upwelled water and create filaments of cold, rich water, which extend offshore on the next meander [*Coastal Transition Zone Group*, 1988]. Closed eddies may be created on either side of the jet by instabilities of the flow, but in the meandering jet model, the jet is the primary structure and source of energy. An important characteristic of the meandering jet is the presence of water in the core of the jet from far upstream, which would not be the case for squirts and would occur only haphazardly in a mesoscale eddy field. The biological implication of the meandering jet structure is that nutrients and biomass from the coastal ocean tend to remain on the inshore side of the jet.

The question is not whether the flow field associated with the cold filaments is always only a squirt, eddy, or meandering jet. We expect to find examples of each of these types of flow in a complex system such as the California Current. The question is whether there is a coherent pattern in the evolving mix of these regimes. The seasonal cycle is of special interest: if features in the velocity field appear for only part of the year, the primary structures may be indicated by the seasonal progression.

Previous observations have not resolved the large-scale synoptic structure of the currents well enough to differentiate between these models. The California Cooperative Oceanic Fisheries Investigations (CalCOFI) sampling was too coarse to define the filaments and seldom extended north of San Francisco. Long-term means based on the CalCOFI data off central California show a broad, meandering southward flow in summer [*Wyllie*, 1966; *Hickey*, 1979; *Lynn and Simpson*, 1987; *Chelton*, 1984], rather than the offshore-flowing jets that appear in more detailed surveys of the same area [*Chelton et al.*, 1988]. Off northern California, however, fields for April, July, and September [*Wyllie*, 1966; *Hickey*, 1979] show strong offshore flow near Point Arena (39°N) similar to features found in later studies. A finer-scale survey of the coastal ocean from 37°N to 43°N was made in May 1977 [*Freitag and Halpern*, 1981]. Although only the region within 100 km of the coast was surveyed, the dynamic height field shows a continuous jet, flowing from north of Cape Blanco to offshore-onshore jets south of Cape Mendocino, Point Arena, and Point Reyes.

More detailed measurements off northern California were made during the 1980s as part of the Coastal Ocean Dynamics Experiment (CODE) and the Ocean Prediction Through Observations, Modeling, and Analysis (OPTOMA) program. The CODE measurements in summer 1981–1982 were concentrated over the shelf, but two offshore surveys in July 1981 and July 1982 found strong offshore transports of cold water; the surveys did not cover a large enough area to determine whether a similar onshore flow occurred [*Flament et al.*, 1985; *Kosro and Huyer*, 1986]. During the OPTOMA program between 1982 and 1986, a large number of expendable bathythermograph (XBT) and conductivity-temperature-depth (CTD) surveys were made in a variable region extending 100–300 km offshore and alongshore off northern California with good seasonal coverage [*Rienecker and Mooers*, 1989*a*]. The surveys of the region farther offshore often have the appearance of a mesoscale eddy field, but midsummer fields from off Point Arena in 1984 and 1986 show a jet very much like that found in the July 1988 CTZ surveys [*Rienecker and Mooers*, 1989*a,b*]. South of the region sampled by the CTZ experiment, recurrent eddies have been documented by a number of studies [*Simpson et al.*, 1984, 1986; *Lynn and Simpson*, 1987].

2. The CTZ Experiment

The region of approximately 37.5°N–41.5°N was studied intensively in 1987 and 1988 [*Coastal Transition Zone Group*, 1988]. Hydrographic surveys of the region within 200 km of the coast were conducted in February, March, May, and June 1987 [*Kosro et al.*, this issue; *Hayward and Mantyla*, 1990; *Ramp et al.*, this issue; *Hood et al.*, 1990, this issue] and June–July 1988 [*Huyer et al.*, this issue; *Chavez et al.*, this issue; T.P. Stanton et al., Upper ocean response to a wind relaxation event in the coastal transition zone, submitted to Journal of Geophysical Research, 1990]. A fluorometer was mounted on the CTD to measure chlorophyll and related pigments on most cruises [*Schramm et al.*, 1988]. Repeated microstructure measurements were made on alongshore transects across filaments [*Dewey and Moum*, 1990; *Dewey et al.*, this issue]. Most of these surveys included continuous 300-kHz acoustic Doppler current profiler (ADCP) measurements, referenced using LORAN-C navigation data to produce absolute velocities in the upper 200 m [*Kosro et al.*, this issue]. Lagrangian measurements of the current structure were provided by surface drifters [*Paduan and Niiler*, 1990; *Brink et al.*, this issue; M.S. Swenson et al., Drifter observations of the dynamical and thermodynamical structures in a cold filament off Point Arena, California, in July 1988, submitted to Journal of Geophysical Research, 1990, hereinafter referred to as Swenson et al., submitted]. Sequences of satellite images were used to direct some of the field measurements and also to estimate surface currents by objective and subjective feature tracking [*Tokmakian et al.*, 1990]. Finally, numerical and laboratory models were used for process studies of coastal ocean circulation [*Haidvogel et al.*, this issue; *Allen et al.*, this issue; *Narimousa and Maxworthy*, 1989] and for hindcast studies using observations to provide the initial and boundary conditions for the model [*Walstad et al.*, this issue].

3. Results From the CTZ Experiments

3.1. *Large-Scale Seasonal Patterns in Wind and SST*

Wind forcing off northern California during 1987–1988 generally followed the normal seasonal cycle of mean

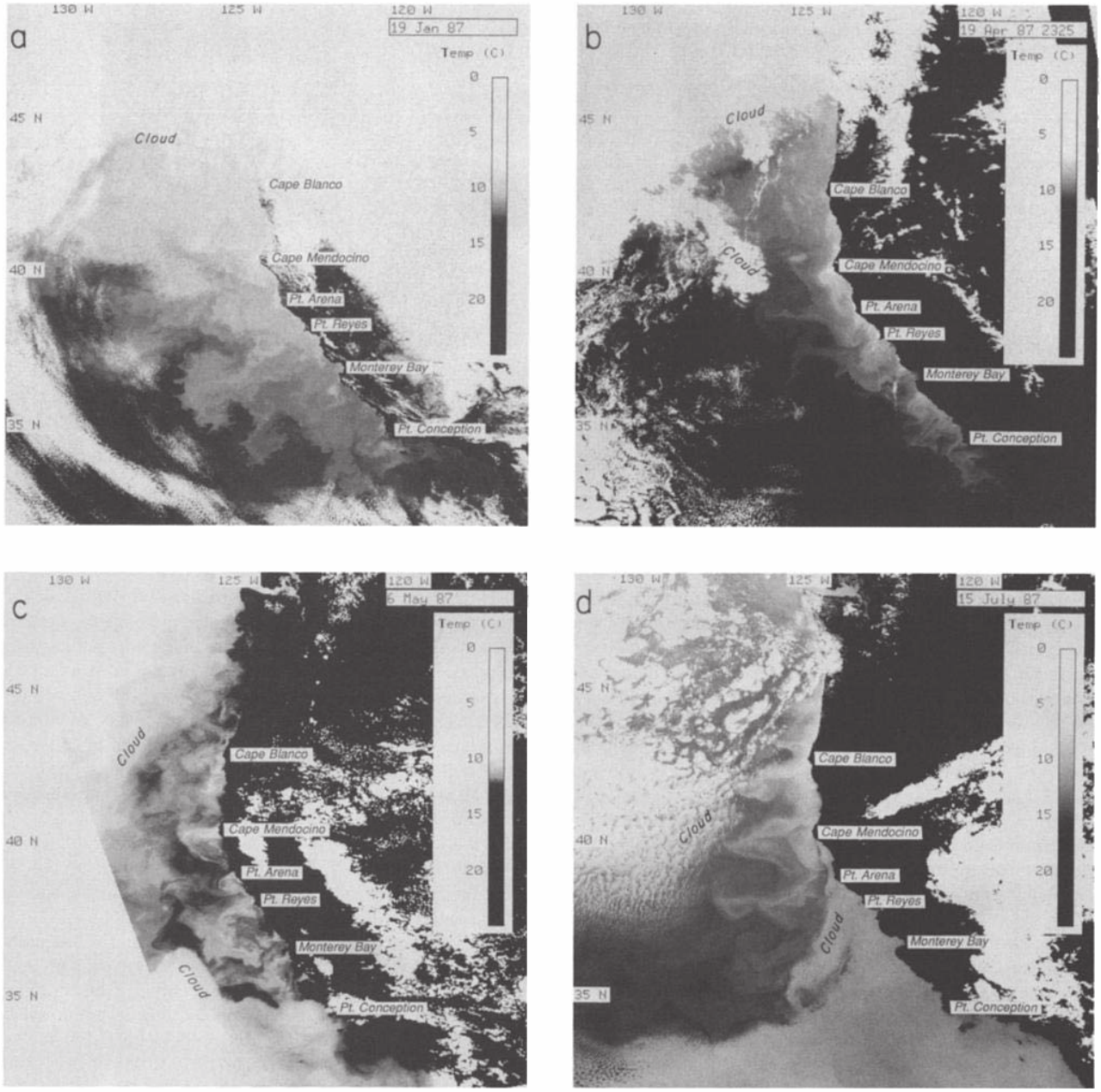

Fig. 2. Satellite SST images from the AVHRR sensor (note the changes in gray scale shading: (*a*) January 19, 1987; (*b*) April 19, 1987; (*c*) May 6, 1987; (*d*) July 15, 1987; (*e*) July 16, 1988; (*f*) October 18, 1987.

northward winds in winter and southward winds in spring–summer, with more variable winds in winter [*Hickey*, 1979; *Huyer*, 1983; *Strub et al.*, 1987*a*]. During the survey in February 1987, there was a period of strong southward winds for approximately 10 days, followed by a return to more northward winds, as is shown by *Kosro et al.* [this issue]. From mid-March to July 1987, winds were upwelling-favorable everywhere, with occasional relaxations and reversals. In 1988, winds were less upwelling-favorable north of Cape Mendocino until mid-June, after which winds were strongly upwelling-favorable everywhere, providing stronger and more persistent wind forcing off northern California from mid-June to mid-July 1988 than was experienced during the March–June 1987 field season.

An overview of the seasonal development of the cold filaments in 1987 and 1988 is provided by satellite SST fields over the large-scale California Current system (34°N–49°N). Six of these are shown in Figure 2. *Kosro et al.* [this issue] present a similar sequence with a greater number of images over a smaller region in 1987.

The image from January 19, 1987 (Figure 2*a*), is clear in the region south of 44°N and east of 128°W, where weak structure with large scales is evident in the offshore SST field. There are local regions of colder water near some capes, but no narrow filaments. Images from February 1987, shown by *Kosro et al.* [this issue], depict similar structure in early February, as well as a band of cold water next to the coast in late February (similar to the early

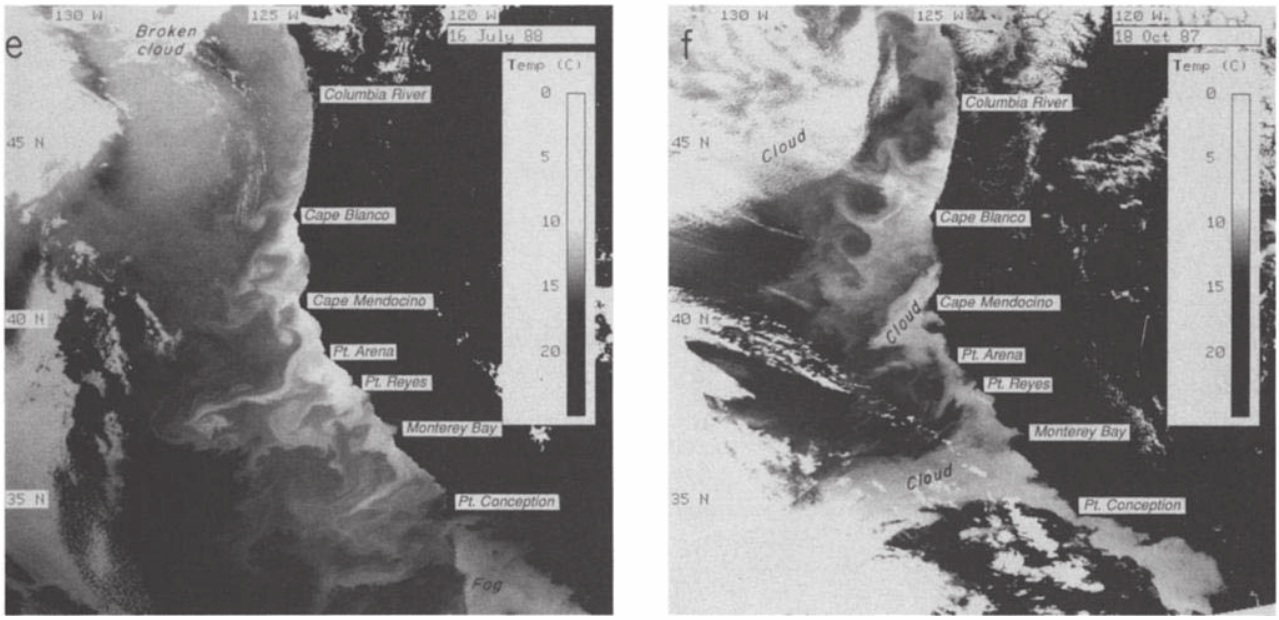

Fig. 2. (continued)

spring images in Figure 2*b*), which resulted from the period of strong southward winds in February. Images from March and April of both years are similar to the image from April 19, 1987 (Figure 2*b*), with colder water in a band within 100–150 km of the coast south of Cape Mendocino.

Images from May of both years are similar to that from May 6, 1987 (Figure 2*c*). Small (100 km), cyclonic filaments are found off Cape Blanco, Cape Mendocino, and Point Arena. These begin to develop in April (Figure 2*b*). Longer filaments extend from Point Reyes and from Point Sur (south of Monterey Bay). Features change fairly rapidly in May–June of these two years, both increasing and decreasing in length, as described in detail below.

By mid-July of both years (Figures 2*d* and 2*e*), filaments extend up to 300 km offshore from Cape Blanco, Cape Mendocino, and Point Arena. South of Point Arena in July 1988, there are several smaller filaments. North of Cape Blanco in May–July of both years, the region of colder temperatures narrows to the north and disappears near the mouth of the Columbia River (46.2°N), as in Figure 2*e*. Features north of Cape Blanco increase in size during the second half of summer and fall, as is demonstrated by the image from October 18, 1987 (Figure 2*f*), which shows longer filaments north and south of Cape Blanco. The scalloped edge of the region offshore of the cold water is suggestive of a line of anticyclonic eddies, as depicted by *Simpson et al.* [1986].

3.2. *Horizontal Fields of Velocity*

The relation between the horizontal velocity field and the filaments can be examined by comparing satellite images of SST with hydrographic fields and with tracks of surface drifters. Figure 3 shows the dynamic height anomaly fields relative to 500 dbar for four surveys in 1987, covering the period March–June 1987. These surveys are described in more detail by *Hayward and Mantyla* [1990] and by *Kosro et al.* [this issue], who show that results from a February survey are similar to those from the March survey. Satellite images (Figure 4) from the same region and period as the surveys show that filaments on the offshore edge of the cold water are associated with the inshore half of the jets, as was also noted by *Hood et al.* [1990] and *Kosro et al.* [this issue]. For example, in the May 18 image (Figure 4*b*), the coldest filament extends offshore at 40.3°N, 125°–126°W and is continuous with a wavy cool filament returning onshore between 40°N, 126°W and 39.5°N, 125°W. Figure 3*c* shows that the more northern filament lies within the southern half of an offshore-flowing jet centered at 40.6°N, 125.5°W, while the more southern filament is in the onshore-flowing jet centered at 39.8°N, 125.5°W. More detailed across-jet transects of surface velocity and temperature for this survey are presented by *Kosro et al.* [this issue].

If we interpret the cold filaments as showing the inshore side of a jet, the combination of satellite images and surveys shows the temporal development of a meandering jet in March–June 1987. The fields show a progression from a small dynamic height range (0.86–0.91 dyn m) in February–March to a large range (0.70–1.00 dyn m) and an alongshore jet with geostrophic velocities of 0.5–0.8 m s^{-1} in May and June. The alongshore jet was already present in mid-March, inshore of the CTZ survey, as was demonstrated by surface drifters which travelled from north of Cape Mendocino to near Point Arena at speeds of 0.1–0.6 m s^{-1} [*Magnell et al.*, 1990]. Interpretation of the April–May dynamic height field in Figure 3*b* is aided by ADCP surface velocities presented by *Hayward and Mantyla* [1990], which show a continuous jet flowing outside of closed eddies found southwest of Cape Mendocino and Point Arena. The May 5 SST field (Figure 4*a*) indicates that the jet meanders approximately 100–150 km offshore of Cape Mendocino.

By May 18, the meander off Cape Mendocino grows sharper and longer, extending 200–225 km offshore (Figure 4*b*). By June 1 (Figure 4*c*), the Cape Mendocino meander has smoothed out and extends only 150 km offshore, while the meander off Point Arena (39°N) has begun to grow. The increasing offshore transport in the cool feature at 39°N (Figure 4*c*) was documented by ADCP data along

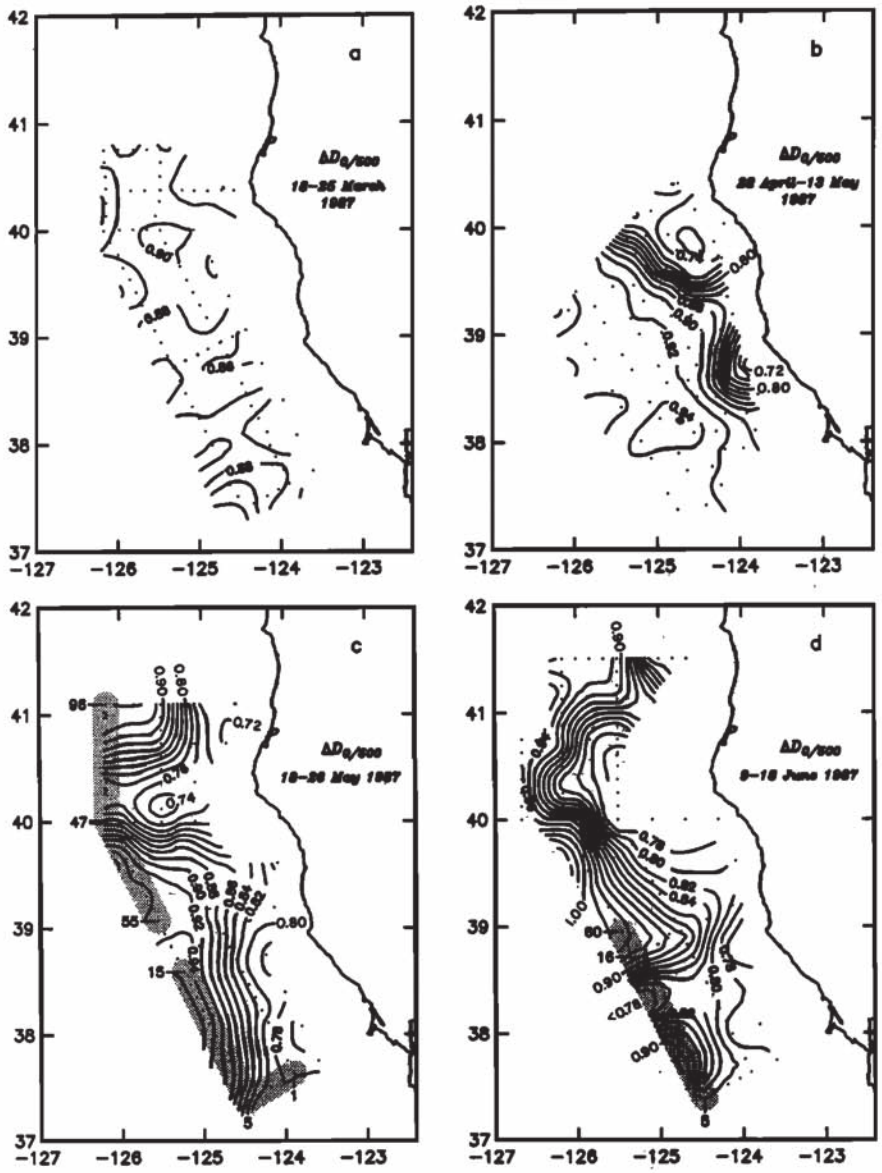

Fig. 3. Fields of dynamic height anomaly relative to 500 dbar from four cruises in 1987 (negative longitudes denote west longitude; contour interval is 0.02 dyn m): (*a*) March 18–25; (*b*) April 28 to May 13; (*c*) May 18–26; (*d*) June 9–18. The shading in Figures 3*c* and 3*d* indicates the location of transects shown in Figure 8.

north-south transects along 125°W (white line in Figure 4*c* [*Dewey and Moum*, 1990]); these show that westward transport in the upper 150 m increased from 2.1 Sv to 3.6 Sv during June 2–5. This could be interpreted as (1) a growing squirt, (2) the northern side of a growing meander, directing more flow into the component normal to the transect, or (3) an eddy that is spinning up. A dynamical interpolation of the flow field between the late May and mid-June surveys, using a quasi-geostrophic (QG) model [*Walstad et al.*, this issue], supports the interpretation of the growing meander. By June 10 (Figure 4*d*) the cool feature off Point Arena extends 200 km offshore to 126°W. The June 10 and 16 (Figure 4*e*) images show cold water being carried offshore and onshore in meanders off Cape Mendocino (39.5°–41°N) and Point Arena (38°–39°N) and offshore to the southwest again south of 38°N, as confirmed by the June 9–18 survey (Figure 3*d*).

Another aspect of the surface flow field is revealed by the tracks of surface drifters drogued at 15 m. Six drifters, released between May 18 and 20, 1987, near 38.1°N, 123.8°W, went north around a small cyclonic eddy off Point Arena that was not resolved by the dynamic height field in Figure 3*c*, and three others went southwest (Figure 5*a*, see also *Paduan and Niiler* [1990, Figure 2*c*]). This closed eddy was resolved in the ADCP data presented by *Kosro et al.* [this issue] (see also Figure 16*a* below). Tracks of similar drifters released on June 17–27 near 38.5°N, 124°W (Figure 5*b*), indicate that the offshore end of the meander between 38°N and 38.5°N (partially resolved by the survey in Figure 3*d*) is near 126°W. These also show that the offshore flow southwest of Point Reyes at 37.5°N, 124.6°W (Figure 3*d*), is the northern side of another meander that extends southwest to 36°N, 126°W. A comparison of Figures 5*a* and 5*b* shows the increase of the offshore extent of the meanders in the jet from 125°W to 126°W during the month between drifter surveys. In Figure 5*b* the drifters from the earlier deployment are seen south of 37°N, circulating slowly inshore of the jet.

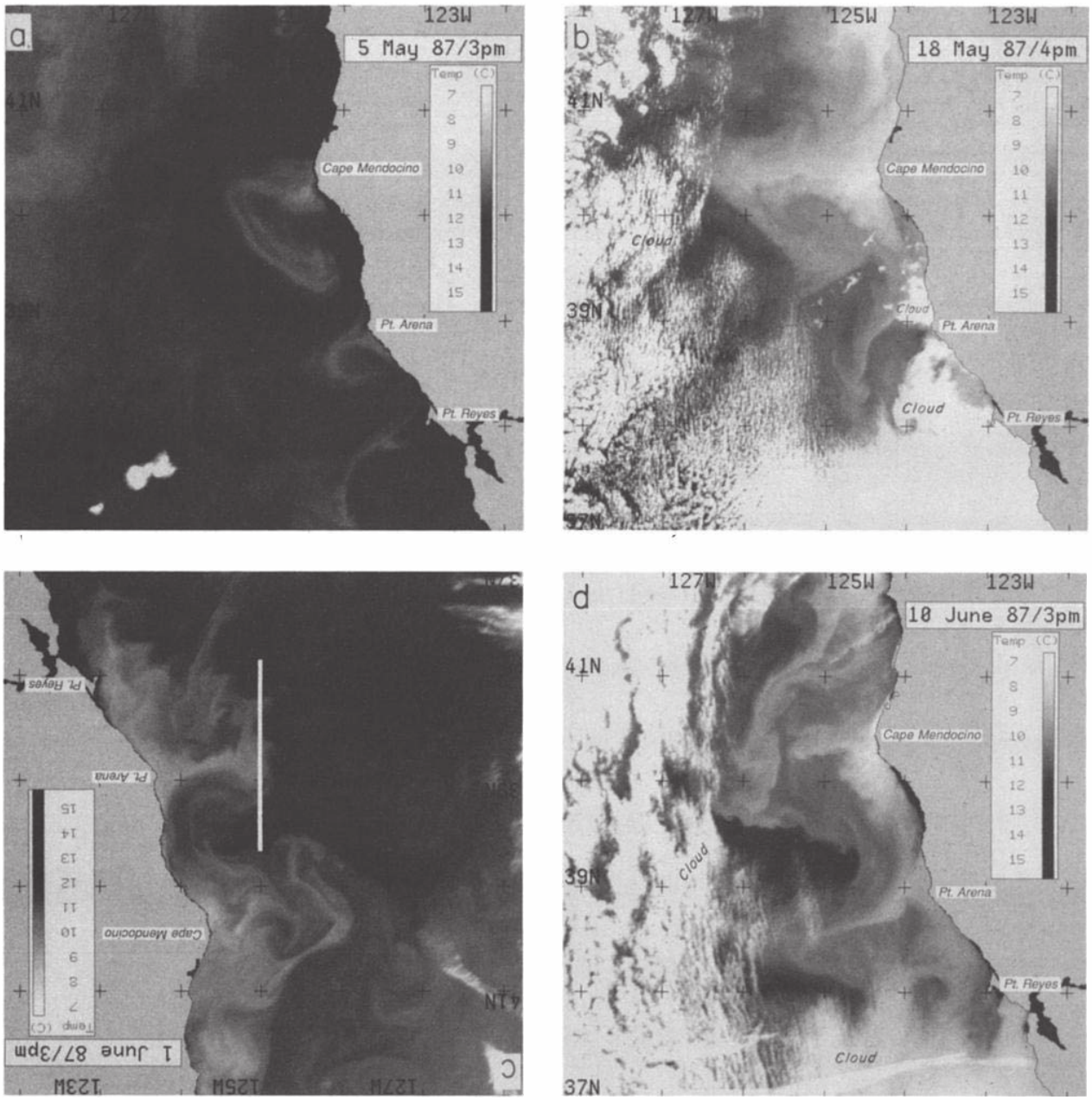

Fig. 4. Satellite SST images: (*a*) May 5, 1987; (*b*) May 18, 1987; (*c*) June 1, 1987 (the white line shows the transect sampled on June 2–5, 1987); (*d*) June 10, 1987; (*e*) June 16, 1987.

The surveys in 1987 did not extend past June, but the July 15, 1987, satellite image (Figure 2*d*) indicates that by mid-July the meander around Cape Mendocino extends again to approximately 40°N, 127°W, and curves back onshore south of Cape Mendocino and then offshore in a large filament extending southwest from Point Arena to approximately 38°N, 127°W. This long, offshore cold filament at 38°N presumably shows the cold water on the inside of the meander at 38°N, which has grown since it was sampled by the drifters in mid-June (Figure 5*b*). It is similar to the feature sampled from June 20 to August 4, 1988 (Figure 2*e*). It is also similar to features seen in July images from most other years and sampled by hydrography in 1981, 1982, 1984, and 1986 (discussed below). Thus we take the 1988 surveys (of a smaller area southwest of Point Arena) to represent a continuation of the general seasonal progression seen in the 1987 surveys.

Figure 6 shows fields of the dynamic height anomaly relative to 500 dbar from three cruises in 1988. The field from July 6–12 in Figure 6*a* is similar to the fields from surveys on June 20–27 and July 13–18, 1988 (see [*Huyer et al.*, this issue] for all five surveys). The primary feature during this month-long period was a fairly stationary jet flowing to the southwest from nearshore just north of Point Arena. *Huyer et al.* [this issue] show that the colder water of the filament lies on the southern half of the offshore jet. Smaller eddies of both signs are present in the slow moving water to the southeast of the jet, and there is an indication of return onshore flow south of the jet. The orientation of the jet in the survey region became

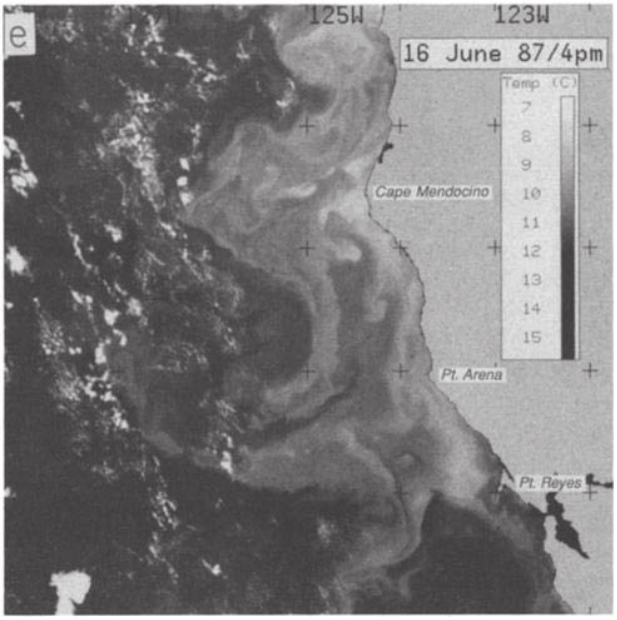

Fig. 4. (continued)

more nearly southward after July 21 (Figure 6*b*), and the jet broadened and weakened by the time of the last survey at the beginning of August (Figure 6*c*).

Surface drifters [*Brink et al.*, this issue; Swenson et al., submitted] from selected periods in June–August 1988 are shown superimposed on satellite images from the same periods in Figure 7. A drifter (labeled R), placed in a filament off Point Reyes at the end of June (Figure 7*a*), followed the filament offshore, circled cyclonically, and then proceeded southward, where it was entrained into a large anticyclonic eddy centered near 124.0°W and 35.7°N, which appears as warm water in the satellite images; it remained in this eddy throughout the end of July (Figure 7*c*). The rest of the drifters (labeled A) were released in the filament off Point Arena (Figure 7*a*). At the end of this filament, most of the drifters turned cyclonically around a "terminal eddy" (labeled E in Figure 7*b*). Some then were carried south in a continuation of the Point Arena jet (labeled A), some became entrained in the terminal eddy, and some leaked off to the northwest (labeled W). Some of the drifters never reached the terminal eddy, but left the jet on its southern side and returned onshore (labeled O). These circled cyclonically off Point Arena (Figure 7*c*) and rejoined the offshore jet.

Near the end of July (Figure 7*c*), the terminal eddy became somewhat cut off from the now more southward jet; some drifters (labeled S) continued south without ever passing around the terminal eddy and meandered back onshore on the north side of the anticyclonic eddy identified by the Point Reyes drifter (R). A month later (Figure 7*d*), the drifter paths show that the terminal eddy had moved to 36.7°N, 127.5°W, approximately 70 km west of its position in late July. Although partially covered by clouds, the drifters show that the anticyclonic eddy at 35.5°N, 123.7°W is near its original location, and they suggest another anticyclonic eddy near 34.5°N, 127.5°W. Southward flow is still found south of the terminal eddy, i.e., south of 36°N between 125°W and 127°W.

Several drifters from the 1988 deployment left the jet and travelled westward as far as 134°W at latitudes between 30°N and 39°N, without encountering another southward jet. Thus the observed jet off Point Arena at 39°N was not one of several similar offshore branches; it was the only such jet at that location and time, although there may have been other jets farther inshore over the shelf and slope. South of Point Arena, multiple cool filaments and drifter

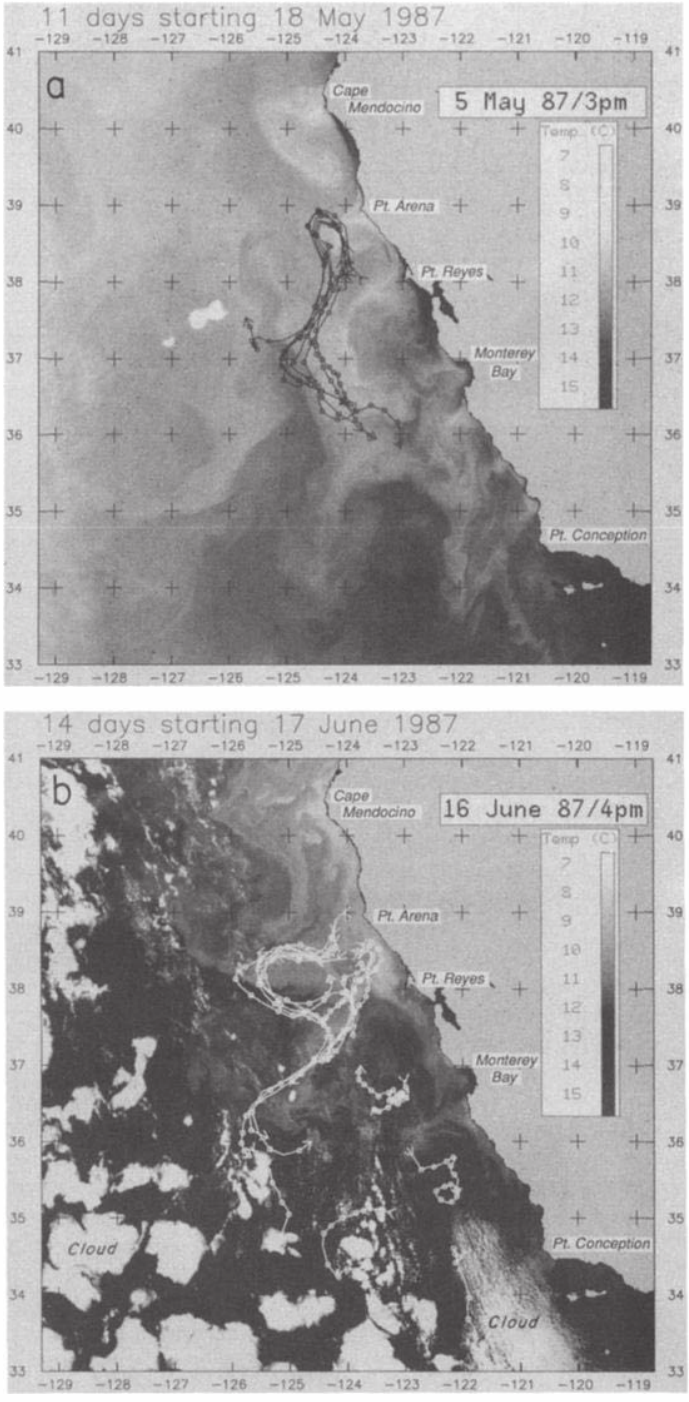

Fig. 5. Surface (15 m) drifter tracks (circles denote 24-hour positions): (*a*) 11-day tracks for drifters released during May 18–20, 1987, overlaid on the satellite SST image from May 5, 1987 (the closest image that was clear over a large area) (circles denote 24-hour positions); and (*b*) 14-day drifter tracks for surface drifters released during June 17–27, 1987, as well as the earlier drifters still in the area, overlaid on the satellite SST image from June 16, 1987.

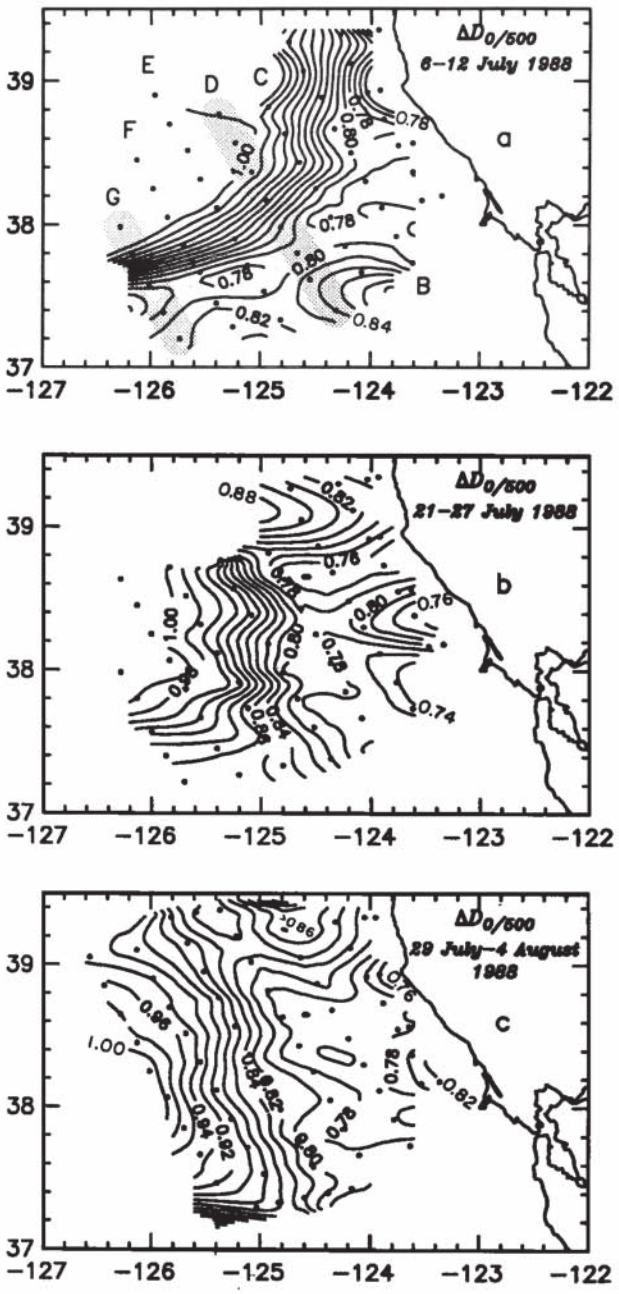

Fig. 6. Fields of dynamic height anomaly relative to 500 dbar from three surveys in 1988 (contour interval is 0.02 dyn m): (*a*) July 6–12; (*b*) July 21–27; (*c*) July 29 to August 4. The shading and letters indicate sections shown in Figure 9.

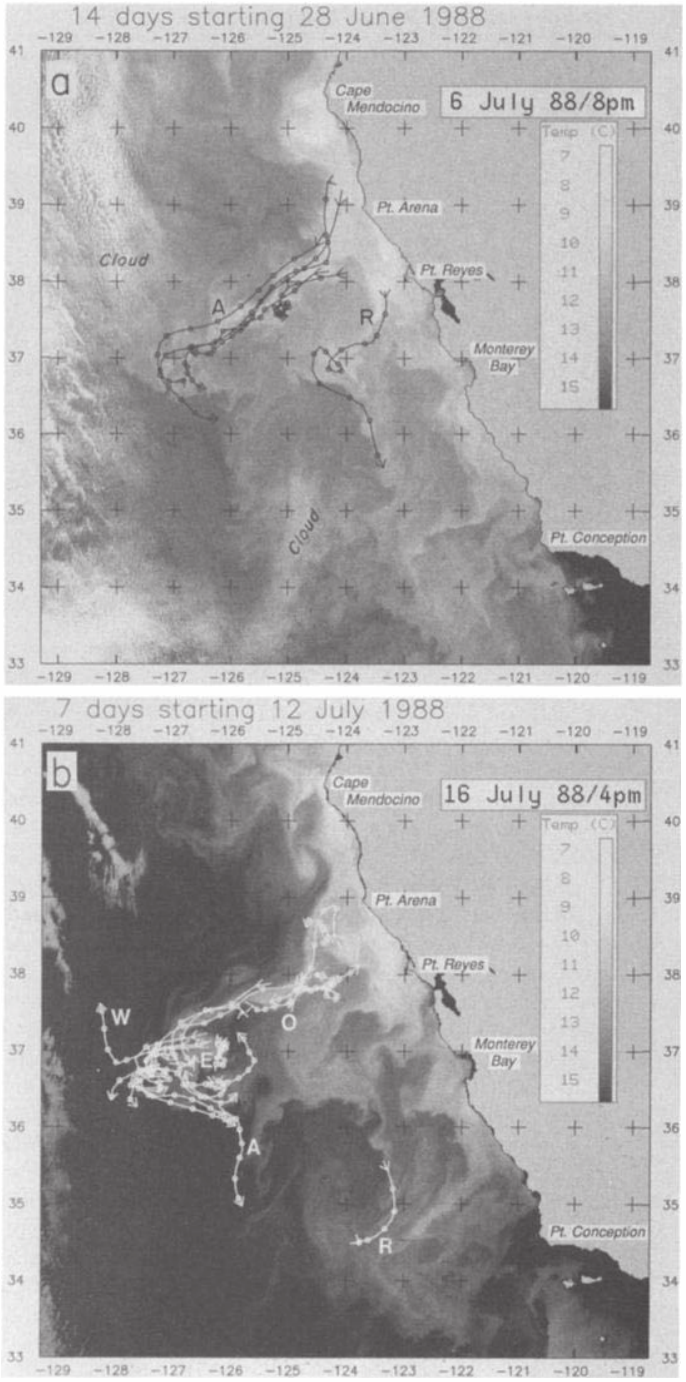

Fig. 7. Surface (15 m) drifter tracks (circles denote 24-hour positions): (*a*) 14-day tracks of drifters starting June 28, 1988, overlaid on the satellite SST image from July 6, 1988; (*b*) 7-day tracks of drifters starting July 12, overlaid on the satellite SST image from July 16; (*c*) 7-day tracks of drifters starting July 25, overlaid on the satellite SST image from July 28; (*d*) 7-day tracks of surface drifters starting August 27, overlaid on the satellite SST image from August 30.

paths inshore of the jet indicate that the transport is not contained in a single jet. Statistical analysis of the drifter motion suggests that the flow south of Point Arena can be characterized by an approximately equal combination of mean southward flow (0.5 m s^{-1}) and an eddy diffusivity that is stronger in the offshore direction (5–8 x 10^3 m^2 s^{-1}) than in the alongshore direction (2–5 x 10^3 m^2 s^{-1}) [*Brink et al.*, this issue].

3.3. *Relation of Velocities to Water Properties*

Examination of the spatial relation between the velocities and the water properties (temperature T, salinity S, nutrients, and biomass) allows us to address two questions:

(1) What is being transported alongshore and offshore at a given location; i.e., are the jets conveyers or barriers for offshore transport?; (2) What are the upstream sources of the water in the jet, as compared with those inshore and offshore of the jet; i.e., are the jets continuous over extensive alongshore distances?

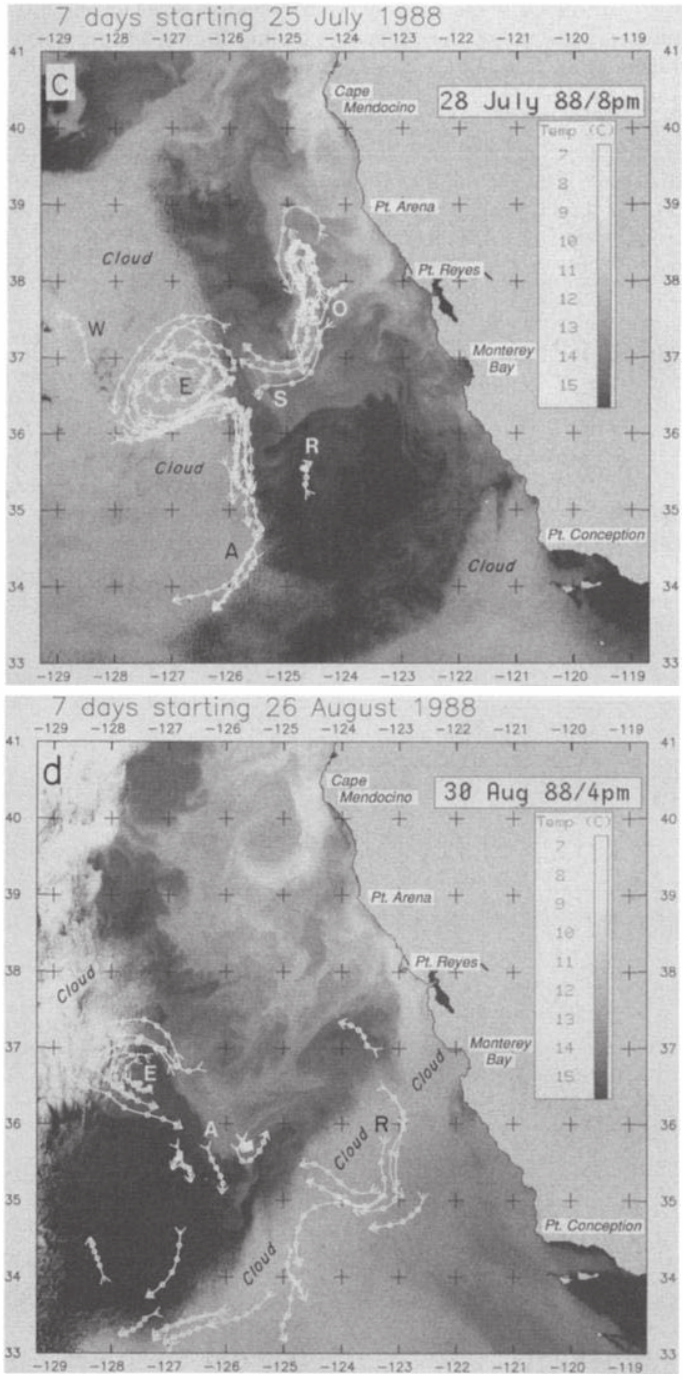

Fig. 7. (continued)

3.3.1. *Surface properties and across-jet sections.* The view that the jets associated with the filaments act as barriers, trapping the colder and richer upwelled water on their inshore side, is most consistent with the surface fields. In early May 1987 (Figure 3*b*), *Hayward and Mantyla* [1990] found a minimum of salinity in a fresh tongue of surface water on the offshore side of the jet. The same pattern was found in a patchy manner in the later 1987 cruises [*Kosro et al.*, this issue] and was consistently found in the jet off Point Arena in June–July 1988 [*Huyer et al.*, this issue]. Thus the outer part of the jets found off Cape Mendocino and Point Arena does not consist of recently upwelled water. A temperature minimum was often found on the inshore half of the jet, sometimes coincident with a salinity maximum and sometimes closer to the velocity maximum than the salinity maximum. Surface nitrate and phytoplankton pigment were highest on the inshore side of the maximum velocities in the jet [*Hayward and Mantyla*, 1990; *Kosro et al.*, this issue; *Hood et al.*, this issue; *Chavez et al.*, this issue], although relatively high values of pigment concentrations (1.0–8.0 mg m^{-3}) occurred in regions on the inshore side of the jet where velocities were 0.2–0.5 m s^{-1} [*Hayward and Mantyla*, 1990; *Hood et al.*, 1990].

Like the surface fields, vertical sections across the jet usually show the highest concentrations of nitrate and phytoplankton pigment inshore of the jet, but they also demonstrate that moderately high values of pigment extend into the inshore flank of the jet and that pigment maxima sometimes appear directly in, or even offshore of, the maximum velocities in the jet. Examples of these different relationships can be seen in vertical sections from the late May 1987 cruise (Figures 8*a* and 8*b*). The sections are located along the southern and offshore boundaries of the survey (Figure 3*c*). In Figure 8*a*, stations 1–5 form a line extending offshore (roughly east-west) and stations 6–15 extend roughly north-south, along the southern part of the farthest offshore line (approximately 150 km from the coast). The vertical line in Figure 8*a* divides the offshore and alongshore sections. The viewer is effectively looking offshore toward the southwest corner of the survey. Figure 8*b* shows the northern part of the same offshore boundary, where it cuts across the sharp meander off Cape Mendocino (Figure 3*c*). The viewer is looking offshore. The ADCP velocities at the top of the figures are the components normal to the sections, defined positive poleward and shoreward.

Along the southern boundary (Figure 8*a*, sampled on May 18–19), water flows out of the survey region to the southwest along a strong salinity gradient, with coldest temperatures (<12°C) and highest pigment concentrations (>1.5 mg m^{-3}) directly in the core of the jet (we note again that the pigment concentrations used in the present paper are derived from fluorometer measurements, as described by *Schramm et al.* [1988]). Station 5 is near 37.4°N, 124.5°W, where a cold filament can be seen in the June 1 satellite image of Figure 4*c*. On the northern half of the meander off Cape Mendocino (Figure 8*b*, sampled on May 23–26), the strongest offshore velocity (0.5 m s^{-1} at station 91) is in a strong gradient of salinity (32.75–33.25 psu) and in the coldest water (<12°C) on the northern side of the domed structure. The onshore jet is on the southern side of the domed structure in water where surface salinity is less than 33.0 psu (with patches less than 32.75 psu) and the temperature has a strong horizontal gradient. The narrow temperature minimum at station 88 is near 40°N, 126°W, where the wavy cold filament in Figures 4*b* and 4*c* flows back onshore toward the southeast, after curving cyclonically around the end of the meander. A phytoplankton pigment maximum (>2.0 mg m^{-3}) straddles the offshore velocity maximum in the upper 50 m, with local maxima north (offshore) of the offshore-flowing jet (station 93) and on the inshore sides of the velocity maxima (stations 88 and 90). The pigment maxima are between 20 and 30 m deep. Thus regions of maximum biomass (1.5–3.0 mg m^{-3}) appear inshore, within and offshore of the jet 150

km from the coast (Figure 8*b*) in a meander that extends approximately 225 km offshore of Cape Mendocino, before continuing within the jet out of the southwest corner of the survey region off Point Reyes (Figure 8*a*).

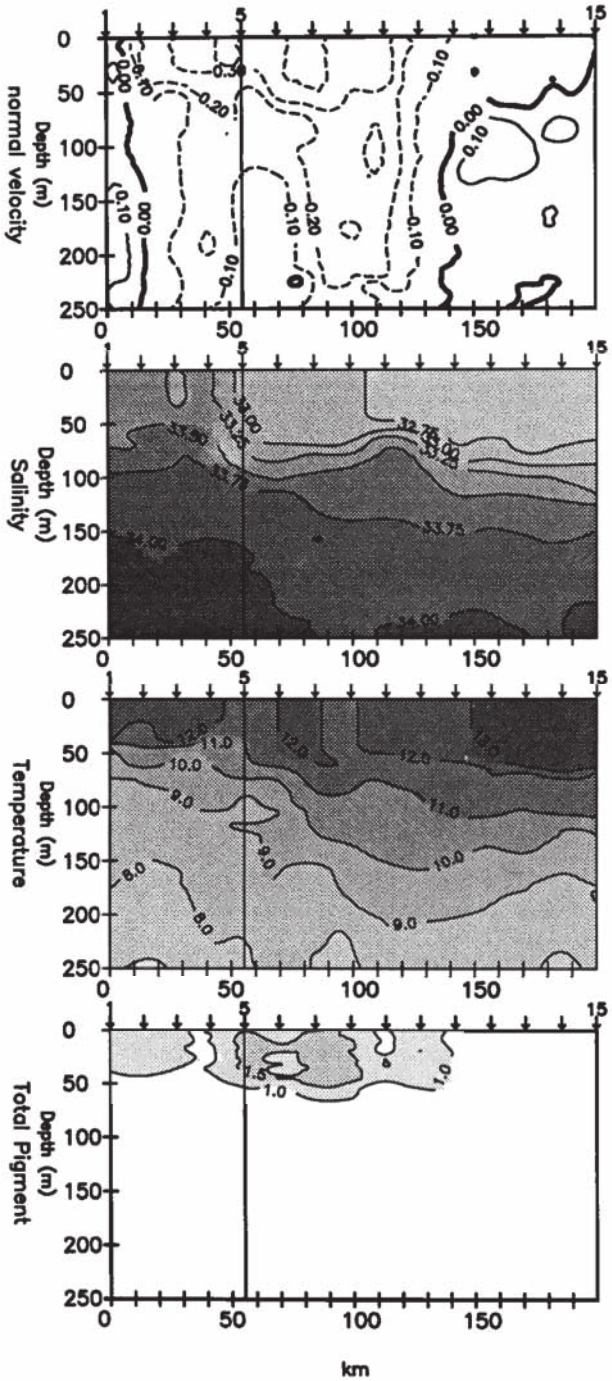

Fig. 8*a*. Sections of (top to bottom) ADCP velocity, salinity, temperature and total pigment concentration (derived from the fluorometer) along the southwest border of the survey on May 18-19, 1987. Stations 1–5 form a cross-shelf transect, and stations 5–15 form an alongshore transect, with the viewer looking toward the south and offshore (see Figure 3 for transect locations). The velocity is the component normal to the transects, defined to be positive poleward and shoreward. Contour intervals are 0.1 m s^{-1}, 0.25 psu, 1.0°C, and 0.5 mg m^{-3} for velocity, salinity, temperature, and pigment concentration, respectively. Pigment concentrations below 1.0 mg m^{-3} appear light with no contours, and pigment concentrations above 4.5 mg m^{-3} appear black with no contours.

Figure 8*c* presents a similar north-south section along the southern half of the offshore boundary during the June 1987 survey. These data were collected mostly on June 10 and can be compared closely with the satellite image in Figure 4*d*. The more northern offshore flow (0.6 m s^{-1} at station 15) is near 38.6°N, 125.25°W, and the onshore flow of 0.3 m s^{-1} in the middle of the section (station 11) is near 38.1°N, 124.9°W. There is a narrow temperature minimum in the left flank of the offshore flow and generally cold water between the offshore and onshore velocity maxima, adding strength to the interpretation of a meandering jet along the outer edge of the cold water in the satellite image. The drifter tracks in Figure 5*b* begin a week later and show this offshore-onshore meander to have moved slightly

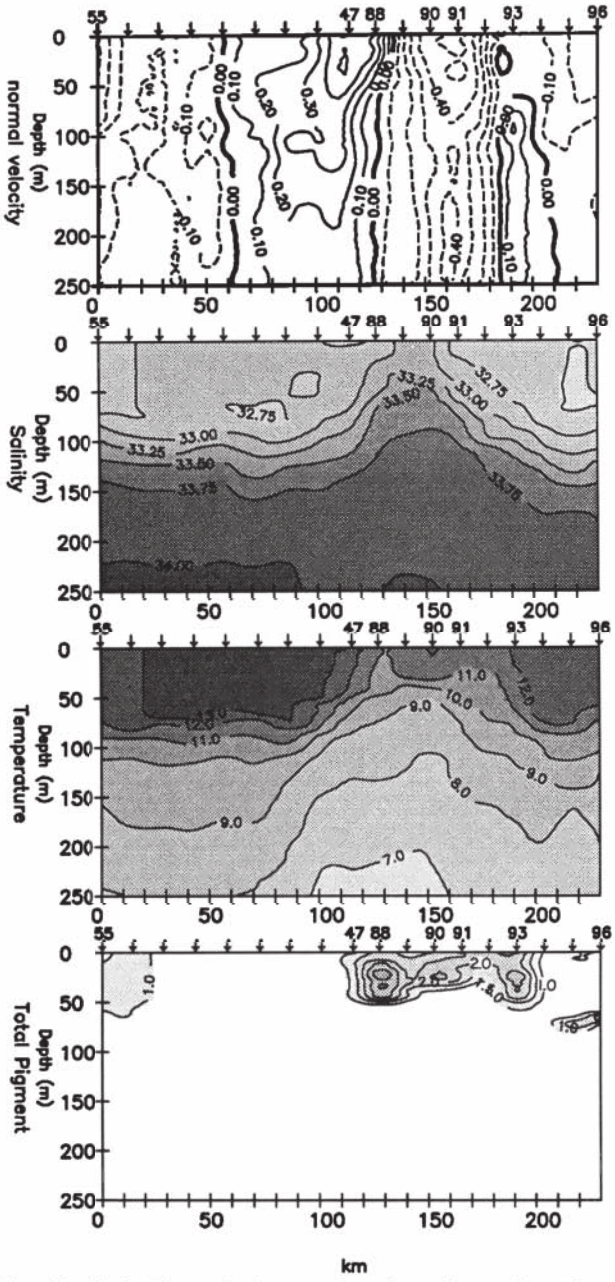

Fig. 8*b*. As in Figure 8*a* for a section along the northwest border of the survey on May 23–26, 1987. Stations 55–96 form an alongshore transect along the line farthest from shore (see Fig. 3), with the viewer looking offshore. The velocity is the component normal to the transects, defined to be positive shoreward.

south in that time. The northern half of this meander corresponds to the feature that grew off Point Arena in early June [*Dewey and Moum*, 1990]. Temperature and salinity show a domed structure similar to that found in the center of the meander off Cape Mendocino in May. Higher phytoplankton pigment concentrations (>1.5 mg m^{-3}) occur inshore of the velocity maxima in regions where the water is moving offshore at up to 0.5 m^{-1} and onshore at up to 0.3 m s^{-1}. The highest pigment concentrations (>4.0 mg m^{-3}) occur south of the more

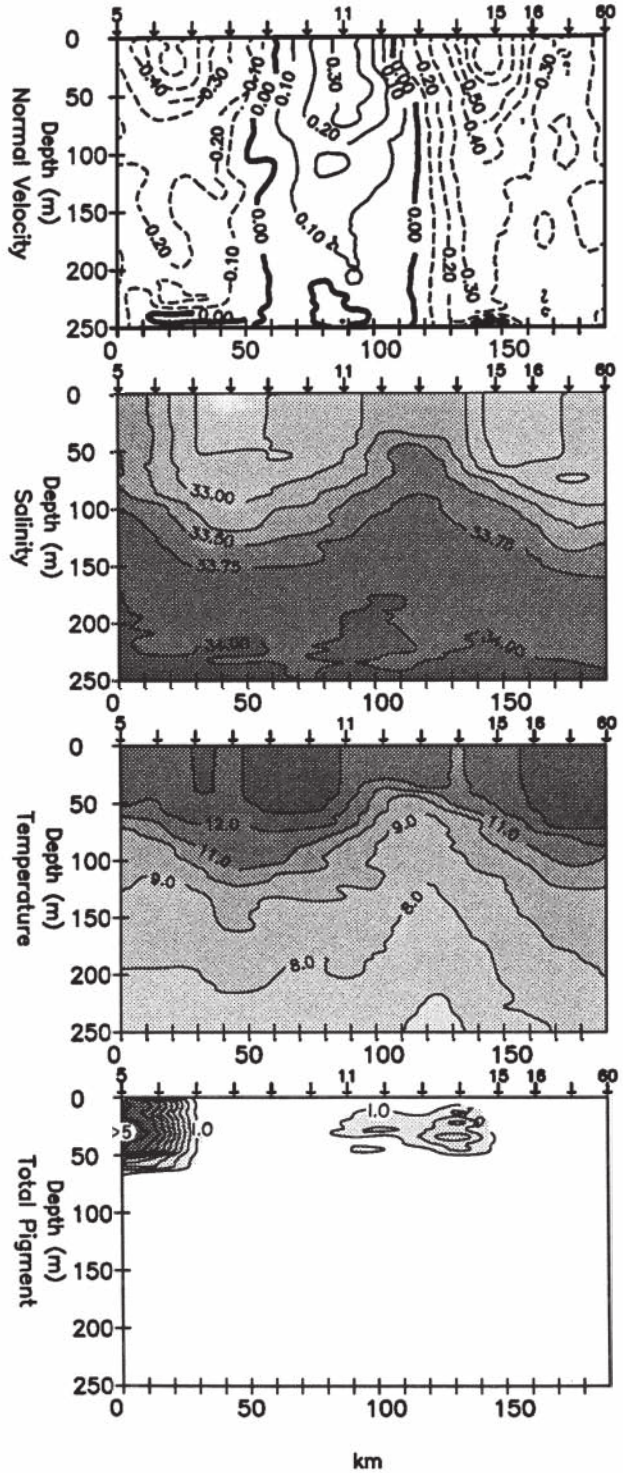

Fig. 8c. As in Figure 8a for a section along the southwest border of the survey on June 10, 1987 (see Figure 3).

southern offshore-flowing jet (stations 5–6, near 37.3°N, 124.5°W), in a region where velocities are greater than 0.3 m s^{-1}. Drifter paths show this to be the inshore region of another meander (Figure 5*b*).

During the repeated surveys of the jet flowing southwest from Point Arena in June–July 1988, the surface fields have features similar to those found in the offshore-flowing northern half of the meanders off Cape Mendocino and Point Arena in the 1987 surveys. A tongue of fresh water is found on the jet's offshore (northern) side, while cold, salty water is found inshore (south) of the jet [*Huyer et al.*, this issue] and the jet lies on the offshore (northern) side of the surface pigment and nitrate gradients [*Chavez et al.*, this issue]. Two across-jet (roughly north-south) transects of onshore velocity, temperature, salinity, nitrate, and total pigment from the July 6–12 survey are presented in Figures 9*a* and 9*b* (see Figure 6*a* for transect locations). As in Figure 8, the viewer is looking offshore and the ADCP velocity is the component normal to the transect, defined positive onshore. These illustrate the distribution of the variables across the jet at distances of approximately 150 km (Figure 9*a*, line D) and 275 km (Figure 9*b*, line G) from the coast, during a period when the jet's position was fairly stationary.

The transects show an irregular domed structure in T, S, and nitrate between the offshore-flowing jet in the north and the weak onshore flow in the south of the transects. The structures are not symmetric about the jet; the velocities and horizontal gradients are weaker to the south. Fresh surface water (<32.75 psu) is found in the northern half of the offshore-flowing jet. Along line D (Figure 9*a*), there is a narrow temperature minimum and nitrate maximum at station 133 (38.0°N, 124.8°W) on the southern side of the offshore jet, where velocities normal to the transect are 0.3–0.4 m s^{-1}. This is also the location of maximum pigment concentrations and the location of a cold filament in the satellite images from July 12 and 16 and drifter tracks in Figures 7*a* and 7*b*. The dome of high salinity appears displaced to the south of the narrow temperature minimum, at the location of zero velocity. Patterns similar to line D were found as far offshore as line F (two transects farther offshore). Farther offshore along line G, the salinity maximum is on the southern side of the offshore-flowing jet, more like the temperature minimum at line D. The minimum of temperature and the maxima of nitrate and pigment are broader, stretching from the southern side of the offshore flow into the northern side of the onshore flow. A shallow salinity minimum is found in the onshore flow at line G. These same patterns were generally found on transects from the June 20–27 and July 13–18 surveys, with the exception that during the July 13–18 survey, minimum surface temperatures increased and maximum pigment concentrations decreased, even though nitrate values remained high.

Repeated sampling (approximately 15 transects) along line D from July 2 to July 16 confirm the picture presented above, with respect to surface variables, with much greater (1 km) spatial resolution [*Dewey et al.*, this issue]. After aligning all 15 of the transects on the density front and averaging over all of the transects, one finds the following qualitative picture, proceeding from south to north: (1) a wide local maximum in salinity where the shallowest (15 m) offshore ADCP velocity is zero, 25 km south of the front; (2) a narrower minimum in temperature north of

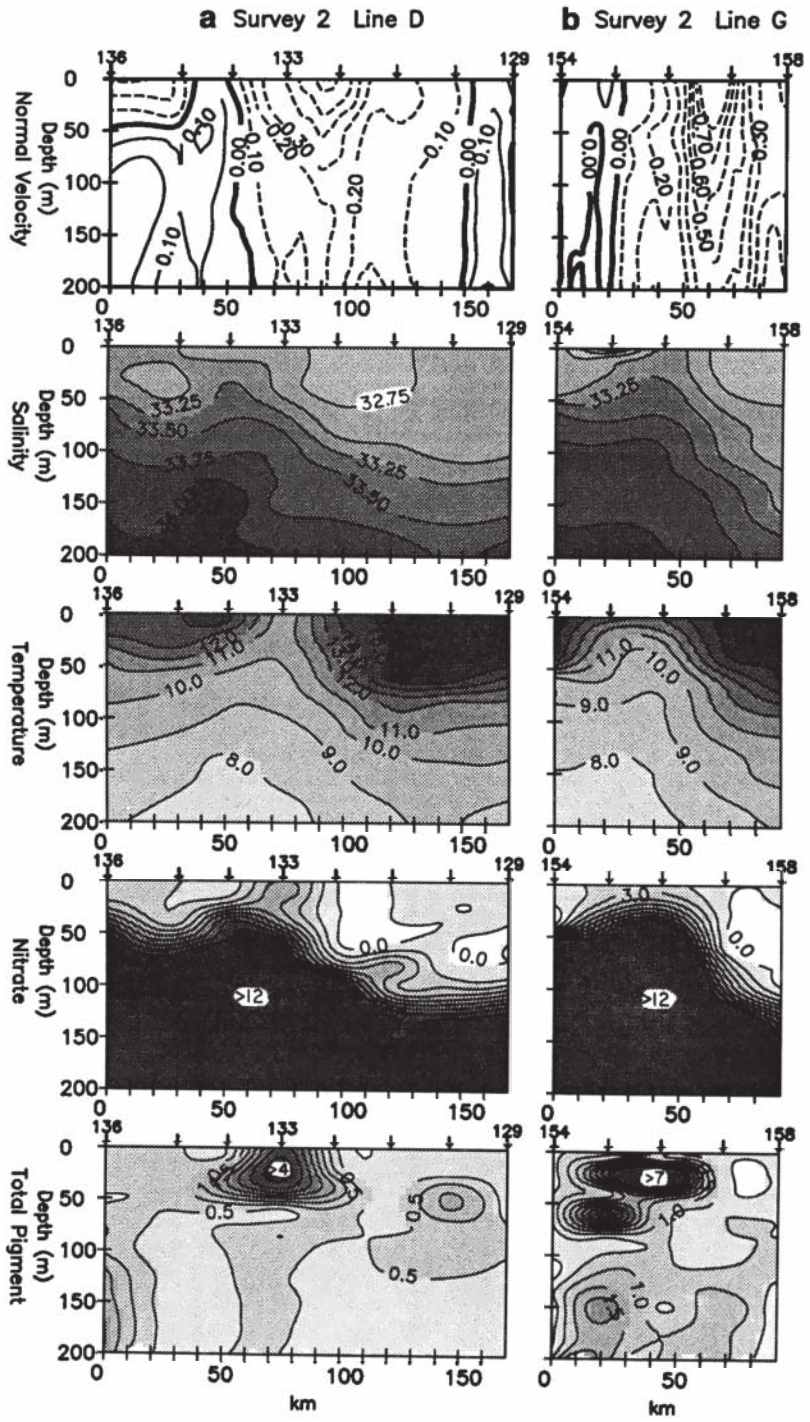

Fig. 9. Sections of ADCP velocity, temperature, salinity, nitrate, and total pigment (derived from the fluorometer) concentration during the July 6–12, 1988 survey. The velocity is the component normal to the transects, defined to be positive shoreward. Contours are as in Figure 8, except that the 0.5 mg m^{-3} contour is shown for pigment, and pigment concentrations above 4.0 mg m^{-3} appear black with no contours. Nitrate is contoured with a 1.5-μM interval and concentrations of nitrate above 12.0 μM appear black with no contours. (*a*) Cross-jet transect along line D on July 9–10; (*b*) Cross-jet transect along line G on July 12. (See Figure 6 for transect locations).

the salinity maximum in water moving offshore at 0.3 m s^{-1}, 10 km south of the front; (3) the maximum offshore velocity (0.6 m s^{-1} in this average) centered 5 km north of the front; and (4) a wide salinity minimum centered 20 km north of the front, in water moving offshore with velocities of 0.3 m s^{-1}. Surface values for velocity, temperature, and salinity during one transect on July 8–9 are presented in the inset of Figure 10*b*, and show some of the same characteristics as the ensemble average.

Although the orientation of the jet in the survey region became more southward during the surveys on July 21–27 and July 29 to August 4 (Figures 6*b* and 6*c*), there continued to be warm, fresh, nitrate-deficient water on the offshore side of the southward jet and cold water with

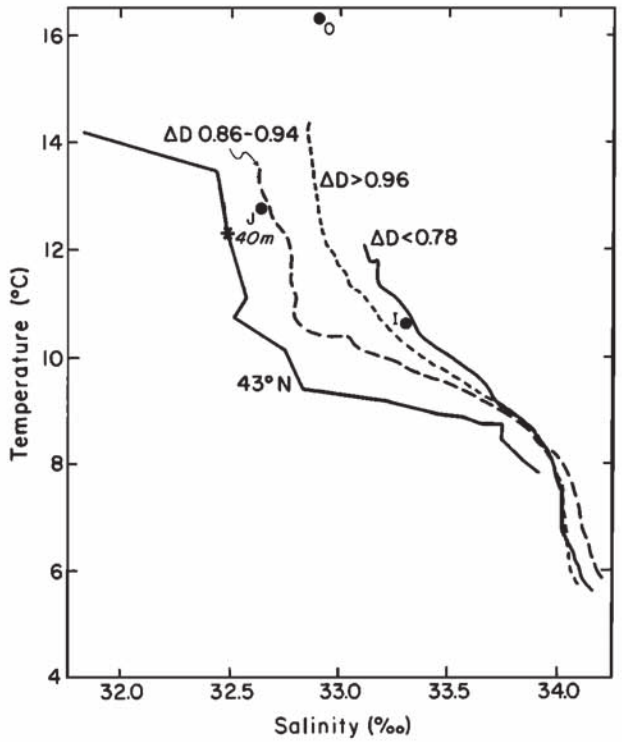

Fig. 10*a*. Mean *T-S* diagrams from the July 6-12, 1988, survey, after *Huyer et al.* [this issue], with profiles averaged according to the surface dynamic height, composited to show profiles judged to be "in the jet" ($0.86 < \Delta D < 0.94$ dyn m); "offshore" of the jet ($\Delta D > 0.96$ dyn m); and "inshore" of the jet ($\Delta D < 0.78$ dyn m). The most offshore profile from north of Cape Blanco (43°N) in June 1987 is also included, and the value at 40 m is indicated by an asterisk. Point *T-S* values used to define the source waters in Table 1 are shown as solid circles (I=inshore, O=offshore, J=jet).

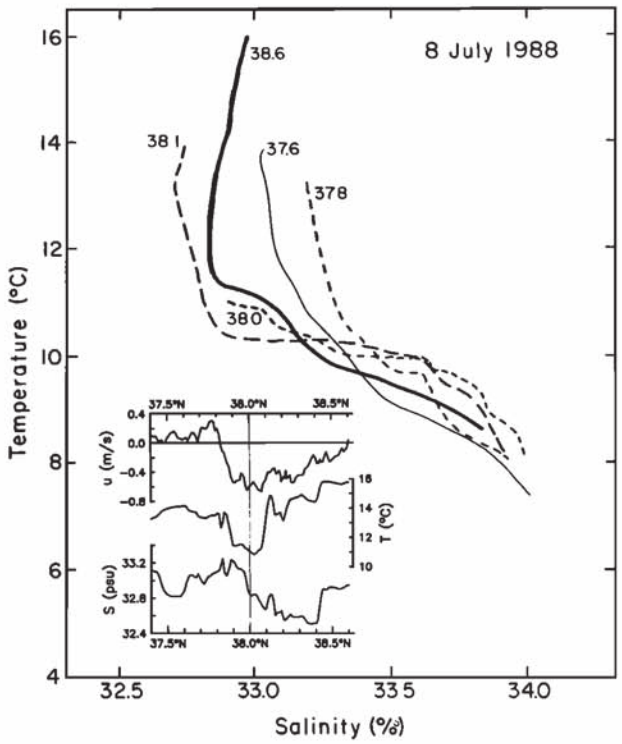

Fig. 10*b*. *T-S* diagrams from July 8-9, 1988, averaged over selected 0.1° latitude bands along line D (see Figure 6*a*). The profiles are labeled with the latitude of the southern boundary of the 0.1° band. The cross-track ADCP velocity at 25 m, the surface temperature, and the surface salinity along the transect are plotted against latitude in the inset.

high nitrate on the inshore side. Pigment values continued to decline to maximum values of only 0.5–1.0 mg m^{-3} during the last survey despite high concentrations of nitrate inshore of the jet, and warmer and fresher water appeared closer to the coast. *Chavez et al.* [this issue] discuss the nutrient and pigment fields in more detail.

3.3.2. *T-S relationships.* One of the most robust results of the 1987–1988 CTZ surveys is the description of a jet that carries along a surface salinity minimum while it separates water of low salinity and nitrate on its offshore side from water of high nitrate and salinity on its inshore side [*Hayward and Mantyla*, 1990; *Hood et al.*, 1990, this issue; *Huyer et al.*, this issue; *Kosro et al.*, this issue; *Chavez et al.*, this issue]. High values of pigment are associated with the inshore characteristics but may also appear directly in the jet or even offshore of the jet in a patchy manner. In trying to relate this structure to the larger-scale California Current, the question arises as to the source of the water masses directly in and separated by the jet. The cold, salty, and nutrient-rich water is presumably of an upwelled origin, either next to the coast or in situ. The fresh water in the salinity minimum must come from farther upstream.

Huyer et al. [this issue] separate the *T-S* profiles for CTD stations from the 1988 CTZ surveys, based on the surface dynamic height, into offshore ($\Delta D > 0.96$ dyn m), jet ($0.86 < \Delta D < 0.94$ dyn m) and inshore ($\Delta D < 0.78$ dyn m) water. Their results from the July 6–12 survey are shown in Figure 10*a*. The jet water is freshest, followed by the offshore water; both are fresher than the inshore water. Measurements made north of Cape Blanco (43°N) at the end of the June 1987 CTZ survey are plotted in the same figure and show water with salinities near 32.5 psu and temperatures of 10.3°–13.3°C between 30 and 70 m at the station farthest offshore (43.2°N, 125.0°W). These values of salinity are in agreement with historical summer values of salinity north of Cape Blanco [*Huyer*, 1983] and with a survey off Cape Blanco in August 1986, which found salinities of <32.0 psu north of Cape Blanco and < 32.5 psu south of Cape Blanco [*Moum et al.*, 1988]. Mixing of this water from north of Cape Blanco with offshore water similar to that found in the CTZ region would produce water with the *T-S* properties found in the jet.

The most detailed sampling of the water characteristics across the jet during the 1988 surveys is provided by the 15 repeated transects of microstructure profiles every 1 km along line D during July 2–16 [*Dewey et al.*, this issue]. *T-S* profiles (averaged over 0.1° latitude bands) from the microstructure transect on July 8 (similar to the July 9–10 transect in Figure 9*a*) are presented in Figure 10*b*. The alongtrack values of velocity (normal to the transect) at 25 m depth, surface temperature, and salinity for the same microstructure transect are shown inset in the figure. In the region of onshore flow to the south of the jet (37.6°–37.7°N), the *T-S* profile shows intermediate characteristics, similar to those previously attributed to "southern" water by *Rienecker and Mooers* [1989*b*] and *Paduan and Niiler* [1990]. Moving north, in the region where cross-shelf velocities switch from onshore to offshore

(37.8°–37.9°N), salinities are greatest and temperatures decrease (the "inshore" water of *Huyer et al.* [this issue], and "upwelled source" water of *Paduan and Niiler* [1990]). In the region near the maximum offshore velocity (38.0°–38.1°N), the T-S profile shows a cold, nearly isothermal layer in which salinity increases with depth. This is in the narrow temperature minimum at station 133 in Figure 9*a* and the narrow cold filament along the drifter track in the July 12 satellite image (Figure 7*b* at 38.0°N, 124.8°W). At the surface it is fresher than the "upwelled source" water of *Paduan and Niiler* [1990] and fresher than the water found over the shelf (> 33.5 psu) in this region and farther north in August 1988 by *Magnell et al.* [1989*a*]. North of the offshore velocity maximum, but still within the offshore-flowing jet (38.1°–38.2°N), the surface water is warmer and fresher and the T-S profile looks like the fresh "jet" water described by *Huyer et al.* [this issue] and the "northern" water described by *Paduan and Niiler* [1990]. The isothermal surface water between 38.0°N and 38.1°N is very similar to the deeper water in the pycnocline at 38.1°–38.2°N. The salinity minimum extends to 38.4°N. North of this, (38.6°–38.7°N) along line D in 1988, the water is saltier and warmer, like the "offshore" water of *Huyer et al.* [this issue].

The identification of phytoplankton and zooplankton species adds further evidence for the upstream source of the jet and the role of the jet in separating water masses. Sampling along line D in July 1988 found different zooplankton species at locations offshore of the jet, within the core of the jet and inshore of the jet [*Mackas et al.*, this issue]. The jet thus carries within its center zooplankton species not found locally inshore or offshore in July 1988, supporting the presence of water from a more distant upstream source. Likewise, *Hood et al.* [1990] find different phytoplanktonic species on either side of the jet in June 1987. Further identification of the species in specific patches by *Hood et al.* [this issue] shows that a deep patch of pigment directly in the jet at 70–100 m depth at 41.5°N in June 1987 is similar to the species found inshore of the jet, in upwelled water, and not the species found in the deep pigment maximum offshore of the jet. Since this patch is below the euphotic zone, they conclude that it has been entrained into the jet and subducted from somewhere inshore and farther upstream. Evidence for subduction within the offshore-flowing jet sampled in 1988 is also provided by *Kadko et al.* [this issue] and *Washburn et al.* [this issue].

3.3.3. *Weighted least squares water mass analysis.* In an attempt to quantify the distribution of source water in the CTZ surveys, the weighted least squares (WLS) water mass analysis of *Mackas et al.* [1987] is used. In this analysis, one specifies values of parameters (temperature, salinity, tracer concentrations) for a number of source water masses. The method determines the best fit of each water parcel to the source characteristics. Each parcel is described as the sum of fractions of the source water types. The sum of the fractions is forced to equal 1.0, and no fraction is allowed to be less than zero. The method weights the parameters by a combination of the variability caused by the measurement error and by uncertainties in the source definitions. A measure of the reliability of the fit is provided by a chi-square test. The method works best with conservative, independent parameters and requires that the number of parameters be as large as the number of source water types (preferably larger). During the 1988 cruises, five variables were used: temperature, salinity, nitrate, silicate, and phosphate, all measured at discrete depths [*Chavez et al.*, this issue].

We are interested in the upper 100 m of the water column, where none of these parameters are strictly conservative (salt may be more conservative at this time of year in this region). Rather than trying to identify distant sources in this nonconservative region, the WLS method was applied with the goal of determining the extent to which the different water masses remained coherent over the month and a half period of surveys. The source definitions used values measured during the July 6–12, 1988, survey at a depth of 40 m (where temperature is somewhat more conservative than at the surface) at three different stations that were judged to be "in" the jet, "offshore" of the jet and "inshore" of the jet. The values are shown in Table 1, and the T-S values are plotted in Figure 10*a* (solid circles). Considering only T-S, the "inshore," "jet," and "offshore" water are similar to the values defined by *Huyer et al.* [this issue].

TABLE 1. Water Mass Source Definitions

	Station Sources					
	Station	T, °C	S, psu	NO_3, μM	PO_4, μM	SiO_4, μM
Inshore	117	10.3	33.3	12.00	1.40	8.93
Jet	115	12.5	32.6	0.01	0.50	2.15
Offshore	143	16.1	32.9	0.11	0.44	2.57

Figure 11*a* shows the fraction of each of the water types found at 40 m depth over the domain of the July 6–12, 1988 survey. Overlaying the surface dynamic height fields shows that "jet" water stays mostly within the jet, with "offshore" and "inshore" water found appropriately offshore and inshore. There is a fairly large amount of patchiness. Examination of the chi-square statistics show these distributions to be significant at the 90% level in regions where jet or "offshore" water represents more than 50% of the water. The regions where inshore water represents the majority of the water are less significant. Application of the WLS analysis to the other surveys at 40 m depth, using the source definitions from the July 6–12 survey, yields similar results. The fields from the June 20–27 and July 13–18 surveys, when the jet was oriented like the July 6–12 survey, are not shown but look like Figure 11*a*. The fields from the July 21–27 and July 29 to August 4 surveys, after the jet has become more north-south, are shown in Figures 11*b* and 11*c*. Even though the jet has shifted position, the water identified as "jet" coincides with the 0.8–0.9 dyn m contours in Figure 6, with a similar amount of patchiness.

The primary result of the WLS analysis is to show the presence of water within the jet during all five surveys that can be distinguished in an objective way from water farther inshore and offshore. Although the properties of the jet water are patchy in space, they do not change much over the month and a half period of surveys. This supports the interpretation of the biological data and the

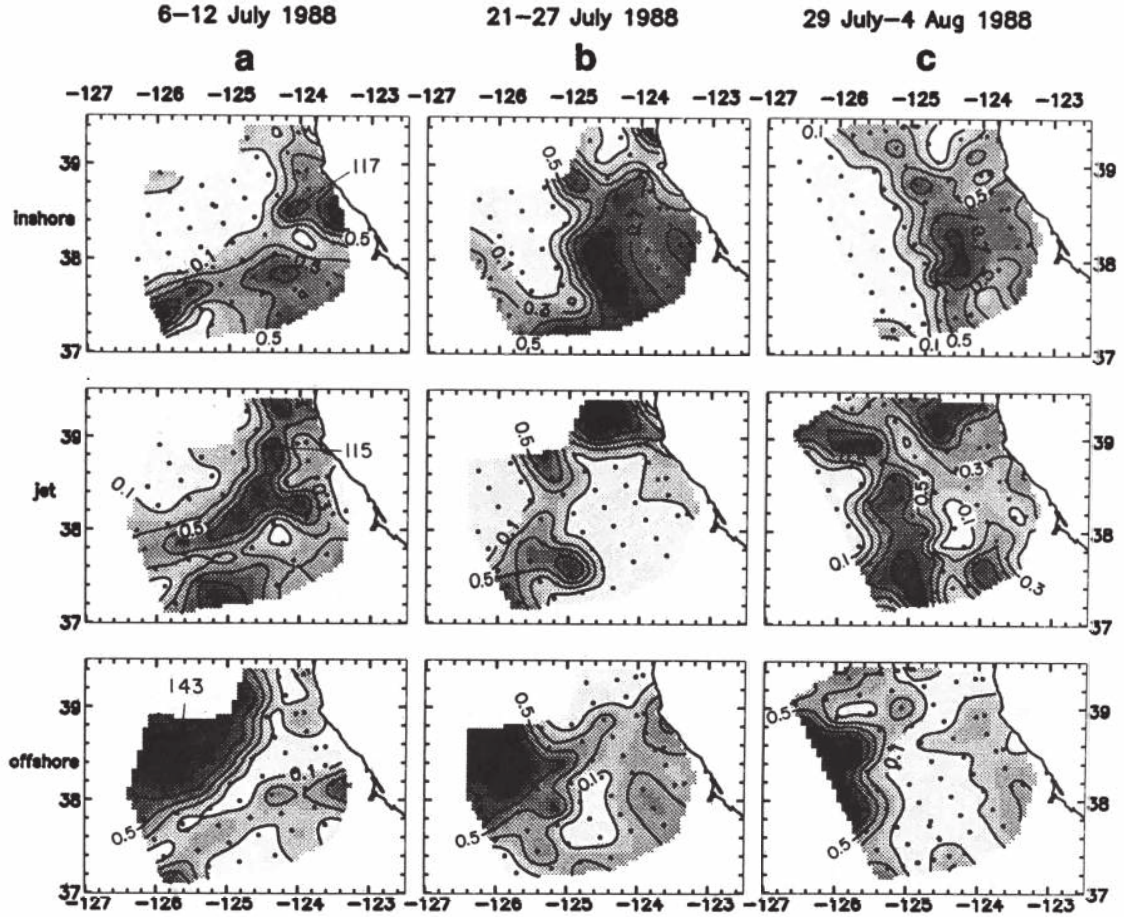

Fig. 11. Horizontal distributions at 40 m depth of the three water types defined by the source characteristics in Table 1 for the three surveys shown in Figure 6. Units are fractions of the water contributed by each source. The locations of the stations (117, 115, 143) used to define the three water types during the July 6–12 survey are shown. The first contour shown is 0.1 and the contour interval is 0.2. (*a*) July 6–12, (*b*) July 21–27, (*c*) July 29 to August 4.

simpler T-S analysis. It also demonstrates graphically the degree of patchiness, indicating intermingling of water types upstream of the survey. These results are similar to the isopycnal analysis by *Huyer et al.* [this issue].

3.4. *Satellite-Derived Flow Field*

A final tool in the analysis of the surface velocity field is the use of sequential advanced very high resolution radiometer (AHVRR) images to infer patterns of motion [*Vastano and Borders*, 1984; *Emery et al.*, 1986; *Kelly*, 1989; *Tokmakian et al.*, 1990]. To determine whether a continuous flow can be traced from Cape Blanco to the Point Arena jet and beyond, a set of 11 clear images from July 16–18, 1988, has been animated, displayed in sequence. This period came at the end of a month of persistently strong upwelling-favorable winds, at the beginning of a week-long wind relaxation [*Huyer et al.*, this issue]. The animation allows us to map the patterns of motion over the 3-day period in a qualitative sense, rather than quantifying the velocities. The advantage of the qualitative interpretation of the animation is that the human eye is adapted to detect motion, even when features are rotating and distorting rapidly. The results of the subjective evaluation of the flow field over this 3-day period are shown in Figure 12. Arrows depicting the qualitative direction of the flow field (not the magnitude of the velocities) are overlaid on the image from July 16, covering the region from 34°N to 46°N. There are no arrows in regions where the direction of flow could not be clearly determined.

Starting in the north at 44°N, the cold coastal features appear to move southward and offshore. The cold water north of Cape Blanco (43°N) flows offshore and separates to form a rapidly rotating cyclonic eddy that moves southward over the 3 days. The colder coastal water south of Cape Blanco also flows to the southwest and eventually extends off Cape Mendocino at 40°N, 126°W. Inshore of this flow is a more complex region that shows northward motion of the warm water and southwestward motion of the cold water north of Cape Mendocino, which eventually merges with the outer flow from Cape Blanco. There is a divergent pattern at 40°N, 126°W, where some of the flow "leaks" offshore and the rest returns onshore. The onshore flow at 40°N turns both north and south, the southward branch flowing into the jet off Point Arena. A mass of cold water emerges south of Cape Mendocino near 39.8°N. This has the appearance of a squirt, as defined at the beginning of the paper, and may be related to the observed wind relaxation. It carries cold water offshore and terminates in opposing vortices, cyclonic to the south and anticyclonic to the north. The cyclonic eddy moves to the south and hits the outer side of the jet near 39.0°N, 124.5°W, where *Huyer et al.* [this issue] suggest it may have influenced the

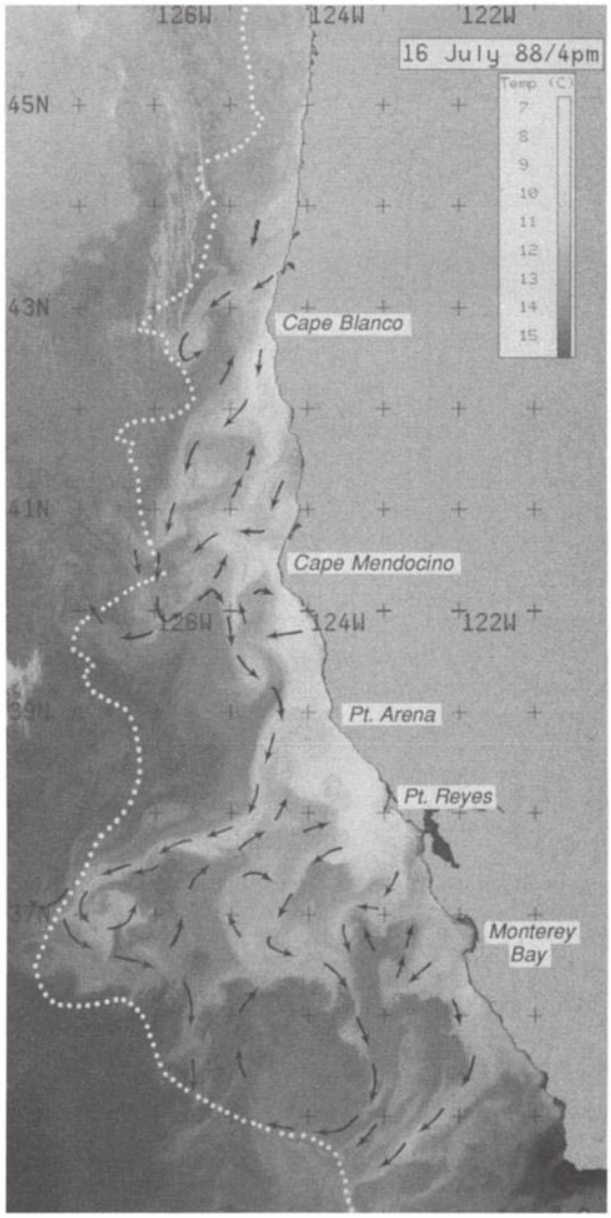

Fig. 12. The subjectively determined (by PTS) July 1988 flow field, from an animation of 11 images on July 16–18, 1988, superimposed on the satellite SST field from July 16. The black arrows depict the direction of the flow, not the magnitude of the velocities. The white dotted line traces the path taken by a surface drifter in September–October 1984 [*Thomson and Papadakis*, 1987]. Although the drifter was from a different year and month than the July 1988 satellite images, it traces out a path similar to the outer edge of the region of cold filaments in the July images.

reorientation of the jet, which occurred at about this time. Offshore of the squirt, the animation shows southward flow that connects the Cape Mendocino meander to the Point Arena jet. Thus a continuous flow can be traced from Cape Blanco to the Point Arena jet, along the outer margin of a much more complex flow field. Water leaves and enters the jet along the path of the jet, suggesting mixing and intermingling of the jet with surrounding water, which would contribute to the observed patchiness of the downstream water mass characteristics.

Starting at the base of the Point Arena filament, the flow is largely as depicted earlier by the 1988 drifter study (Figure 7), with extra details where there were no drifters. The jet terminates in an eddy with moderately rapid rotation. There is some leakage off the northwest corner of the eddy and motion around the eddy and then to the south. Some onshore flow to the south of the jet can be seen, as can offshore flow in several other filaments along the coast to the south. Anticyclonic rotation is evident in the large eddy sampled by the Point Reyes drifter (Figure 7) at 35°N–36°N, 123°W–125°W. For comparison, the path of a satellite-tracked surface drifter which travelled from Vancouver Island (49°N) southward along the coast in September–October 1984 is included in Figure 12 to show that drifters at other times have followed a continuous north-to-south path along the outer edge of this same general region ([*Thomson and Papadakis*, 1987], discussed in more detail below).

4. Discussion

4.1. *Comparison With Previous Results*

4.1.1. *Seasonal evolution.* Observations from the CTZ surveys and satellite (AVHRR) data favor the picture of a strong (0.5–1.0 m s^{-1}), narrow jet that appears sometime between March and May and connects the region from north of Cape Mendocino to that south of Point Arena, at least through July. The seasonal increase in the strength of mesoscale meanders and eddies is in agreement with a late-summer maximum in rms sea surface topography found from analysis of a year-long record of Geosat altimeter data in two independent studies [*Flament et al.*, 1989; *White et al.*, 1990].

To verify this seasonal pattern over a longer time period, dynamic height fields were examined from the CODE (1981–1982), OPTOMA (1982–1986), and CTZ (1987–1988) surveys, located within the region 37°N–42°N and offshore to 128°W. The approximate range of dynamic heights (relative to 500 dbar) within each survey has been tabulated and used to form a mean monthly dynamic height range. Most of the CODE cruises were confined to a narrow coastal region and were not used; the OPTOMA cruises that covered small regions were also not used. If more than one cruise was conducted in the same year-month, the largest range was used for that year-month. The mean monthly progression of the dynamic height range is shown in Figure 13 as the solid line, along with the values from the individual surveys. Given the low number of samples available and the differences in the regions sampled by different surveys, only the general trend of a summer-fall maximum and a winter-spring minimum should be considered significant. Thus there is an agreement of the seasonal progression from this longer (8 year) time series with the results from the altimeter data in 1987 and the interpretation of the satellite SST fields in 1987–1988.

Magnell et al. [1989a,1990] present nearshore CTD surveys and drifter deployments around Cape Mendocino from the Northern California Coastal Current Study (NCCCS) in 1987 and 1988. The nearshore hydrography off Cape Mendocino from March 17–19, 1987 (prior to the CTZ survey in Figure 3*a*) shows a jet located approximately 20 km from the coast at 40.4°N, 124.6°W, with a small anticyclonic eddy inshore of the jet. NCCCS drifters released in March of both 1987 and 1988 travelled nearly uniformly south with little meandering, approximately 20–30 km from shore, from north of Cape Mendocino past Point Arena and sometimes as far as Point Reyes, with velocities of up

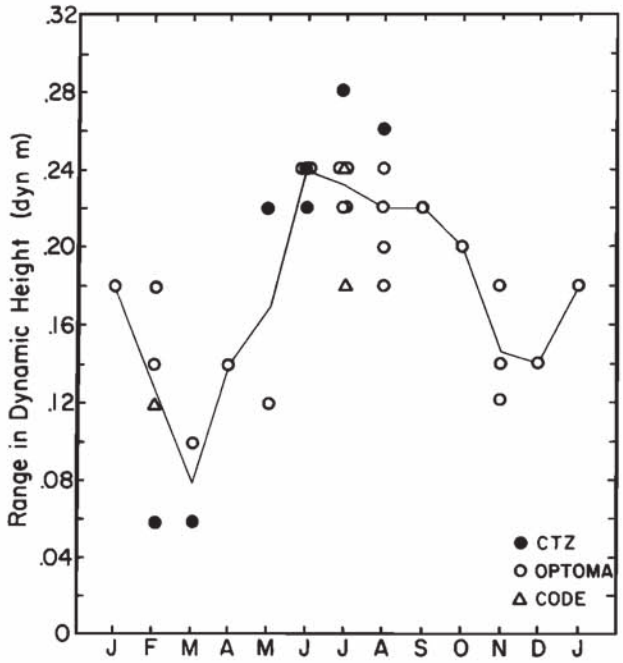

Fig. 13. Seasonal variation in the range of dynamic height maps from the CODE, OPTOMA, and CTZ surveys (1981–1988). The maximum ranges of dynamic heights off 37°–42°N are shown as individual symbols, and the means for each calendar month are connected by the continuous line. Identical values found in different years are indicated by slightly offset symbols.

to 0.6 m s^{-1}. This suggests the presence of a nearshore jet in March of both years.

These observations lead to the hypothesis that the seasonal evolution of the velocity field off Cape Mendocino and Point Arena begins in March or earlier with a jet close to the coast, perhaps along an upwelling front. Offshore movement of a jet associated with an upwelling front is indicated by the CODE data south of Point Arena (near 38.6°N) at the time of the spring transition (March–April) in 1981 and 1982. Current moorings over the shelf [*Strub et al.*, 1987*b*] and CTD cruises [*Huyer and Kosro*, 1987] revealed uniformly southward velocities in an initial response to southward winds. As the wind forcing continued, however, the southward jet moved offshore, and the velocity field over the shelf became more variable. We hypothesize that as the jet moves farther offshore, it separates the more variable region inshore, where upwelled water is found, from the offshore environment. Other jets and eddies may appear inshore of the seaward jet. For example, moored current measurements over the shelf south of Point Arena [*Magnell et al.*, 1989*b*] indicate an inshore jet over the shelf simultaneous with the seaward jet observed offshore in early July 1988 [*Huyer et al.*, this issue]. Similarly, hydrographic sections from the NCCCS survey in August 1988 [*Magnell et al.*, 1989*a*] indicate a southward jet over the shelf and slope at most locations from north of Cape Mendocino to south of Point Arena. These jets can presumably separate from the coast and create multiple jets (each with an associated filament) inshore of the seaward jet, similar to those seen in the drifter tracks and satellite images south of Point Arena (Figure 7). We stress that this hypothesized seasonal progression applies only to the Cape Mendocino and Point Arena region and that further observations are needed to verify it. Farther south, where upwelling-favorable winds are present during most of the year, the temporal evolution of the jet and eddy field remains to be determined.

4.1.2. *Continuity with regions farther north.* Several pieces of evidence suggest continuity of the jet off Cape Mendocino and Point Arena with flow north of Cape Blanco. The satellite image from 6 May 1987 (Figure 2*c*) shows a cyclonic filament off Cape Blanco similar to those off Cape Mendocino and Point Arena, which were observed to be associated with a meandering jet and inshore cyclonic eddies. ADCP data collected after the 9–18 June 1987 survey north of Cape Mendocino show offshore flow north of Cape Blanco, onshore flow south of Cape Blanco, and flow to the southwest between Capes Blanco and Mendocino, leading into the survey region of Figure 3*d* [R. L. Smith, Coastal upwelling in the modern ocean, submitted to Evolution of Upwelling Systems: Miocene to Present, edited by C. P. Summerhayes, W. Prell, and K. C. Emeis, Burlington House Publishers, Bath, 1991]. This flow was along the edge of cold features similar to those in Figure 2*d* and is consistent with the very fresh water (< 32.0 psu) found at the surface on the offshore side of the jet at the northern entrance to the 9–18 June 1987 survey (see Figures 5 and 14 of *Kosro et al.* [this issue]). Animation of the satellite sequence from 16–18 July 1988 (Figure 12) also suggests a continuous flow from Cape Blanco to south of Point Arena. This is consistent with the surface salinity minimum observed in the offshore half of the jet in 1988 and with T-S characteristics in the jet (Figure 10*a*).

Three previous studies provide evidence that the surface currents off Cape Blanco in May, August and September are similar to, and may be continuous with, the meandering jet found off Cape Mendocino. In May 1977, *Freitag and Halpern* [1981] found a jet flowing continuously from north of Cape Blanco to Cape Mendocino, where offshore and onshore flow was seen, similar to the meander found in late May 1987 except displaced slightly to the south. Minimum salinities in the offshore portion of the jet increased from north to south from less than 32.4 psu north of Cape Blanco to 32.6 psu off Point Arena. In August 1986, *Moum et al.* [1988] found a symmetric offshore and onshore current west of Cape Blanco, similar to that found off Cape Mendocino in late May 1987 (Figure 3*c*). Cold water was contained inshore of the jet, which transported fresh water (32.0–32.5 psu) on its outer edge around the cape to the south. Finally, the continuity of the southward flow along the offshore edge of the filament region is supported by the track of a drifter which travelled southward along the coast from Vancouver Island (49°N) in September–October 1984 [*Thomson and Papadakis*, 1987]). The drifter track is shown in Figure 12, superimposed on the July 1988 flow pattern. Starting north of Cape Blanco within 100 km of the coast, the drifter experienced offshore-onshore meanders of 50–100 km amplitude at Cape Blanco, between Cape Blanco and Cape Mendocino, southwest of Cape Mendocino, and southwest of Point Arena. It took approximately a month to travel from Cape Blanco to Point Arena and outlined the system of cold filaments that existed at that time (see *Thomson and Papadakis* [1987] for overlays of the drifter tracks and coincident satellite SST images).

4.1.3. *Across-jet structure and in situ upwelling.* Close examination of the spatial distribution of *T-S* properties along line D in July 1988 (Figure 10*b*) reveals that the

coldest water in the filament (38.0°–38.1°N) is much fresher than coastally upwelled water found inshore of the jet, but is similar to the deeper water found slightly farther offshore in the jet (38.1°–38.2°N). Profiles with a similar isothermal upper region were found to occur in the jet along the path of a drifter moving offshore in the jet [*Kadko et al.*, this issue], although warming at the surface was evident from stations farther offshore than line D. These profiles are very much like those shown by *Rienecker and Mooers* [1989*b*, Figure 8] from the "cold core" of a jet off Point Arena in July 1986. The structure of transects from across the 1986 jet [*Reinecker and Mooers*, 1989*b*, Figure 5*a*] is nearly identical to that found at line D in July 1988 (Figure 9*a*). These T-S profiles suggest that upwelling occurs locally within the jet and that the cold water in the narrowest filaments seen in the satellite images may just be the fresher, northern water found in the offshore half of the jet, without the upper part of the water column.

Several mechanisms have been suggested which would cause upwelling locally within the jet. Model studies by *Haidvogel et al.* [this issue] and *Allen et al.* [this issue] suggest an alternating pattern of downwelling and upwelling on the offshore-flowing and onshore-flowing branches of the jet, respectively. However, the observations along line D come from the offshore-flowing water, where the model predicts downwelling and where *Kadko et al.* [this issue] and *Washburn et al.* [this issue] interpret the observations to indicate subsidence. Whether the narrow region with the isothermal T-S relation in the upper water (Figure 10*b*) could be the remnant of upwelling which occurred during the onshore-flowing branch of the meander remains to be determined.

An alternate mechanism for in situ upwelling is proposed by *Paduan and Niiler* [1990], who use conservation of vorticity to argue that in situ upwelling will take place in a jet which flows downwind, preferentially to the right of the jet (the side of the jet with negative relative vorticity). This would cause upwelling in the fresher water on the offshore side of the jet, consistent with the T-S profiles found in Figure 10*b*. However, the observations along line D do not conform to the theoretical situation, since the wind direction was more cross-jet than along-jet and the observed surface temperature minimum with the isothermal upper layer was found on the inshore side of the velocity maximum. *Paduan and Niiler* [1990] stress that the exact location of the upwelling maximum is sensitive to the distribution of relative vorticity, which is more complicated in the observed jet than in their Gaussian jet. We note that the model studies quoted above have no wind forcing and that the theoretical argument of *Paduan and Niiler* [1990] lacks the three-dimensional dynamics which cause the upwelling and downwelling in the numerical models. Thus although the water properties suggest in situ upwelling of the fresher water as the source of the water in the coldest narrow filament, the mechanisms that might cause that upwelling are not yet known.

4.1.4. *Similarity to other July fields.* The Point Arena jet sampled in June–July 1988 (Figure 6*a*) and the satellite SST fields associated with the jet (Figure 2*e*) are very similar to jets sampled by surveys in 1981 [*Kosro and Huyer*, 1986], 1982, 1984, and 1986 (Figure 14) and July images from 1981–1986 (Figure 15) and 1987 (Figure 2*d*). The dynamic height fields (Figure 14) from July 1982 [*Flament et al.*, 1985], July 1984 [*Rienecker et al.*, 1987], and July 1986 [*Rienecker and Mooers*, 1989*b*] all show a strong offshore-flowing jet extending west or southwest from Point Arena, as sampled in 1988. The satellite images from other July (Figure 15) often show cold water off Cape Mendocino, warm water southwest of Cape Mendocino between 39°N and 40°N, and one or more filaments

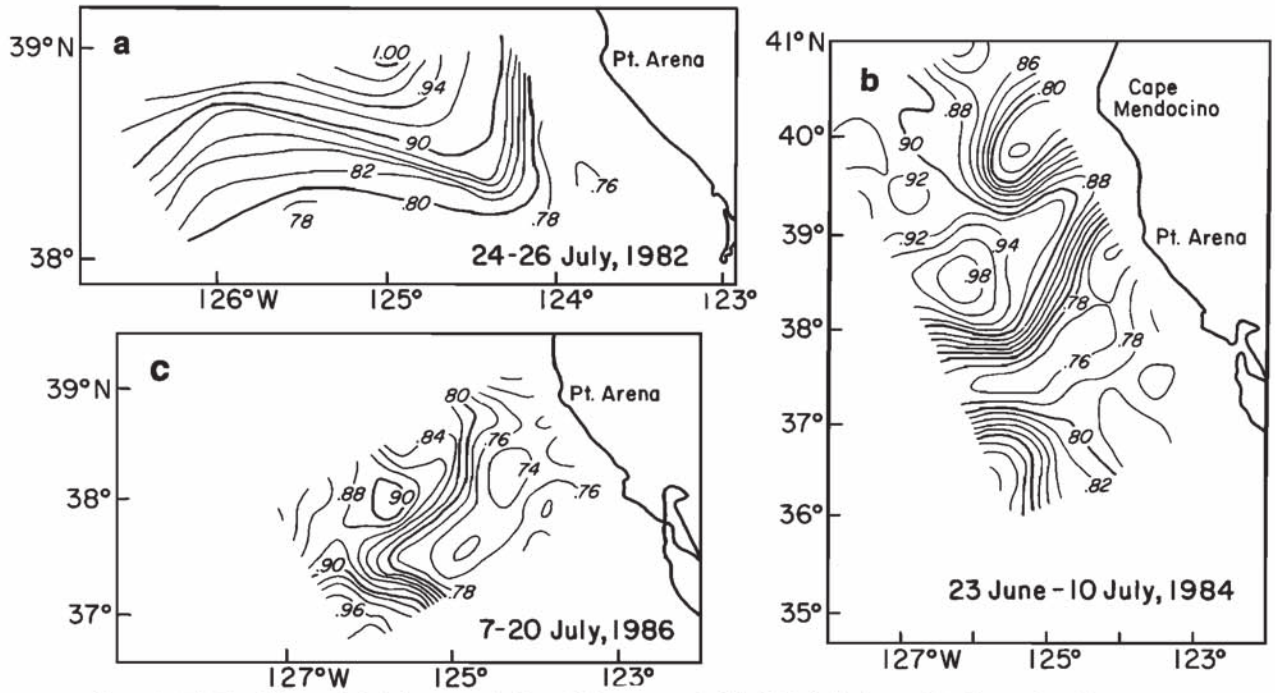

Fig. 14. Fields of dynamic height anomaly from July surveys in (*a*) 1982 (relative to 500 dbar, after *Flament et al.* [1985]), (*b*) 1984 (relative to 450 dbar, after *Rienecker et al.* [1987]), and (*c*) 1986 (relative to 450 dbar after *Rienecker and Mooers* [1989*b*]). The contour interval is 0.02 dyn m.

extending offshore from the region between Point Arena and Point Reyes (38°–39°N). This pattern is consistent with a meander off Cape Mendocino, onshore flow south of the cape, and offshore-flowing jets between Point Arena and Point Reyes. The images also show the degree of interannual variability in the position of the offshore filaments, which may leave the coast anywhere from north of Point Arena (1984) to Point Reyes (1981; see *Kosro and Huyer* [1986] for the 1981 dynamic height field). The 1984 dynamic height field (Figure 14*b*) and satellite image (Figure 15*d*) support the image of a jet that connects the meander off Cape Mendocino to an offshore-flowing jet at Point Arena, which meanders back onshore at 37°N but does not approach as close to the coast as it did between 39°N and 40°N, a pattern similar to that inferred from the drifters and the sequence of satellite images in July 1988 (Figures 7 and 12). The 1986 dynamic height field (Figure 14*c*) covers the jet off Point Arena out beyond the meander's turn to the southeast at 37°N, as is also evident in the satellite image (Figure 15*f*). The OPTOMA surveys in 1984 and 1986 show anticyclonic eddies to the north and west of the jet off Point Arena but also demonstrate that the surface transport in the closed eddies is less than the transport in the continuous jet.

Although the fields from 1984 and 1986 support the model of the meandering jet at the surface, they make it clear that most of the flow that continues south after passing around the cyclonic eddy at the end of the jet off Point Arena does not immediately return close to the coast but continues south, 200–300 km from shore, in contrast to the meander off Cape Mendocino. For the July 1984 jet (Figure 14*b*), this is confirmed by a July 1984 CalCOFI

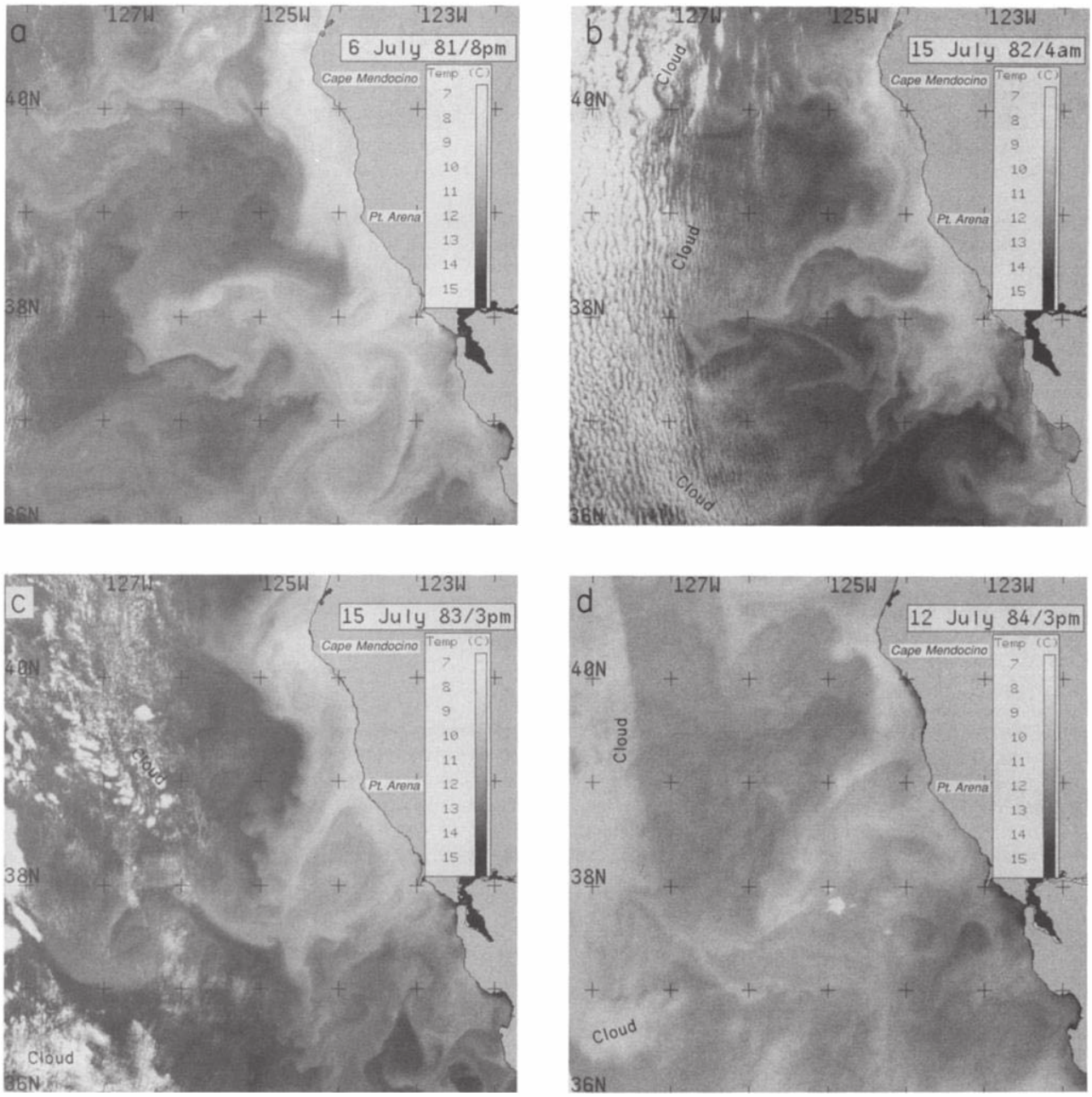

Fig. 15. Satellite SST images from July in other years: (*a*) 1981, (*b*) 1982, (*c*) 1983, (*d*) 1984, (*e*) 1985, (*f*) 1986.

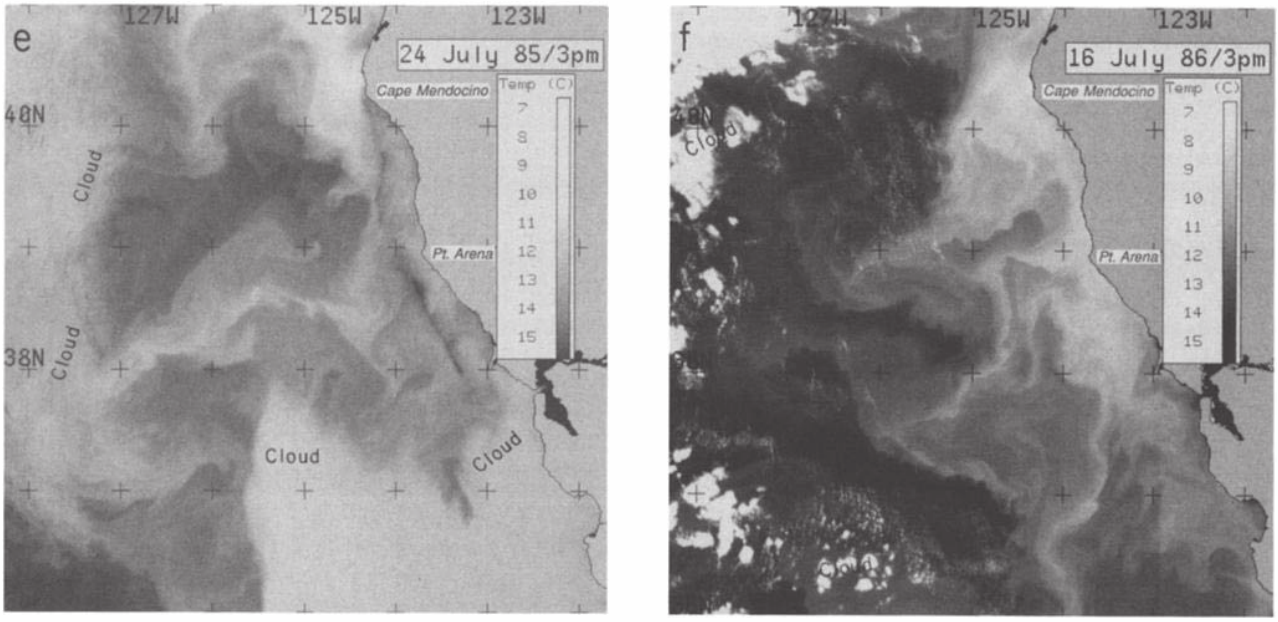

Fig. 15. (continued)

cruise, which showed the main jet extending south of 35°N, 200 km offshore, between anticyclonic (offshore) and cyclonic (inshore) eddies [*Chelton et al.*, 1988]. This pattern is similar to the path taken by drifters in 1988, which continue to the south from 35°N to 33°N between 125°W and 127°W (Figures 7*c* and 7*d*). This is also the path taken by the surface drifter that passed through this region in October 1984 [*Thomson and Papadakis*, 1987] (Figure 12).

4.2. *Comparison With Model Studies*

Although a number of modeling studies have addressed the three-dimensional structure and variability in eastern boundary currents, each study has included only a few of the processes which may influence the circulation patterns in those systems (such as surface buoyancy flux, surface wind stress, wind stress curl, bottom bathymetric features, variable coastline, realistic three-dimensional density and velocity structure, etc.). These "process studies" show the range of responses to isolated processes and often produce velocity fields with meanders and eddies similar to the observations, but they cannot evaluate the relative importance of all the different processes.

For example, *Philander and Yoon* [1982] demonstrate that the response of an eastern boundary current to annual periodic southward wind forcing (with no curl) is a banded structure of currents, associated with westward propagating Rossby waves. These may contribute to the offshore eddy field, as supported by Geosat altimeter data [*White et al.*, 1990]. An alternate explanation of the eddy field is simply the evolution of an initial, alongshore, baroclinic jet (equatorward surface jet over a poleward undercurrent, typical of summer and fall) [*Ikeda and Emery*, 1984; *Haidvogel et al.*, this issue]. These models suggest the importance of coastal topographic features, such as capes, in perturbing the jet. *Pierce et al.* [this issue] and *Allen et al.* [this issue] show that the spatial scale of the most unstable perturbations of jets similar to those observed in the 1987 CTZ surveys is approximately 250 km, a scale which is roughly similar to the separation between capes along the coast of southern Oregon and California. Other models, spun-up from rest by a spatially uniform and steady wind stress, produce a jet which becomes unstable and forms meanders and eddies, without coastal capes or bathymetric features [*Batteen et al.*, 1989; *McCreary et al.*, 1991].

An interesting result is found when *McCreary et al.* [1991] force their model with an annually oscillating (spatially uniform) wind stress. The result is an upwelling front and jet, which develops seasonally and eventually becomes unstable in spring–summer, producing meanders and eddies on both the inshore and offshore side of the jet. In winter, the system decays to weaker, large-scale eddies. Thus seasonal wind forcing alone, with no curl and no coastal or topographic features, can cause the development of an unstable jet, which moves offshore and develops into a jet and eddy field. The scales of the features in the model are sensitive to model parameterizations, especially those involved with horizontal and vertical mixing, which is a point of concern, since these processes are not well represented in numerical models.

Another type of numerical model study uses initial and boundary conditions derived from hydrographic and ADCP surveys to hindcast ("dynamically interpolate") the developing current structure between surveys [*Robinson et al.*, 1986; *Rienecker et al.*, 1987; *Walstad et al.*, this issue]. Such studies provide details of the evolving current structure which extend the observations (within the assumptions incorporated in the models). For example, *Walstad et al.* [this issue] initialize a QG model with the density field and ADCP velocities from a rectangular subregion of the May 18–26, 1987, CTZ survey (Figure 3*c*) and interpolate boundary conditions between that survey and the June 9–18 survey. Figure 16 shows the stream functions from the model at the start, middle and end of the simulation. The initial field shows why some of the

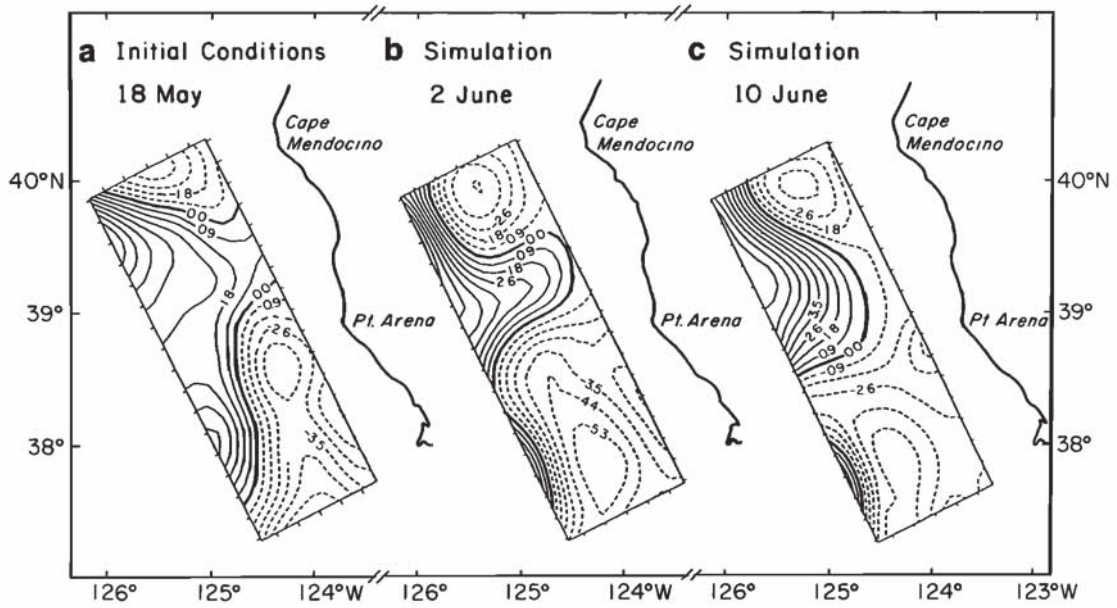

Fig. 16. Streamline fields from the QG model hindcast study of *Walstad et al.* [this issue]. (*a*) Initial conditions, May 22,1987; (*b*) June 2 simulation; (*c*) June 10 simulation.

drifters released at 38.1°N, 123.8°W, went north around the closed eddy of Point Arena and some flowed to the southwest (Figure 5*a*). During the simulation, the onshore flow south of Cape Mendocino becomes a sharper onshore meander between the two capes, while the streamlines off Point Arena begin to bow outward, creating the sharp offshore meander off Point Arena observed in the June 1987 cruise. The growth of the meander off Point Arena around June 2 was observed as the growing cold feature in the AVHRR images (Figure 4*c*) and in the ADCP measurements of increasing offshore transport on June 2–5, 1987, at 39°N, 125°W [*Dewey and Moum*, 1990]. The model demonstrates how the growth of a meander may look like a squirt in satellite images and even in a field survey of a limited domain.

Rotating laboratory tank experiments represent a final type of model. *Narimousa and Maxworthy* [1989] present results from a series of two-layer experiments in a tank that include rotation, surface stress (with and without curl), idealized capes and bottom ridges. Their results suggest that (1) bathymetric ridges produce an offshore-onshore meander coincident with the feature, while capes do not, (2) both ridges and capes produce meanders approximately 100–150 km downstream of the feature, and (3) a positive offshore maximum of wind stress curl produces offshore eddies which draw the coastal water offshore. Although it is tempting to use these conclusions to explain the strong onshore flow south of Cape Mendocino as due to the ridge offshore of the cape, the primitive equation numerical model results of *Haidvogel et al.* [this issue] produces a narrow meander directly offshore of the cape without a ridge in the model bathymetry, contradicting the first conclusion from the laboratory model.

These studies show that depending on the choice of model parameters and forcing, a number of models can produce features that are similar to certain aspects of the observations. At this point, however, none of the model results have demonstrated conclusively which physical processes are responsible for generating the different features observed in the California Current system.

4.3. *Biological Implications*

The CTZ surveys provide evidence that off Cape Mendocino and Point Arena in May–July, the observed jet separates water masses and biological assemblages at the surface and carries nutrients and biomass along on its inshore flank and sometimes within its core. Thus one important implication of the observed structure is that the gradient in biological properties between the richer nearshore and oligotrophic offshore regimes is often concentrated in a narrow frontal region across the jet. Processes which produce cross-jet transport will move biomass and nutrients from the inshore to the offshore environment, where they may be left by meanders and cutoff eddies.

A phytoplankton pigment maximum is often found on the inshore half of the jet as it flows both offshore and onshore (Figures 8 and 9). The net effect of the meanders on offshore transport of biomass depends on the biological processes and vertical motions which occur during the meanders. In a drifter-following experiment during July 1988, which extended beyond the normal CTZ survey region, *Kadko et al.* [this issue] and *Washburn et al.* [this issue] document the subsidence of patches of high pigment concentrations as the drifter moved offshore, at subsidence rates of up to 25 m day^{-1}. Before the drifter reached the end of the filament, pigment concentrations near the drifter were vastly reduced from inshore values and nitrate values were undetectable down to 100 m. It is not clear, however, whether this was true everywhere at this distance from shore or whether the drifter simply missed a patch of pigment such as seen along line G in July 1988, 275 km from shore (Figure 9*b*).

One of the more detailed examinations of the evolution of biological processes within a jet meander is presented by *Abbott et al.* [1990], who discuss fluorometer measurements and water samples collected on a drifting buoy which

sampled the offshore-onshore meander at 38°N in June 1987, shown in Figure 5*b*. During the first 2 days of offshore motion, phytoplankton pigment concentrations (as inferred from strobe-stimulated fluorescence) increased, and nitrate plus nitrite concentrations decreased, indicating phytoplankton growth. At the same time, the initially large concentration of nonfluorescent material decreased substantially. This material covaried with the pigment concentrations, implying that a large proportion of it was biological detritus, which sank out of the upper water column in the first few days of offshore transport. Pigment concentrations then decreased during the rest of the offshore motion, reflecting zooplankton grazing and/or subsidence. By the time the drifter reached the offshore terminus of the meander, there was a strong diurnal cycle of fluorescence around a steady mean value, indicating a balance between daytime growth and nighttime grazing. These results apply to the surface and do not take into account the subsidence described by *Kadko et al.* [this issue] and *Washburn et al.* [this issue].

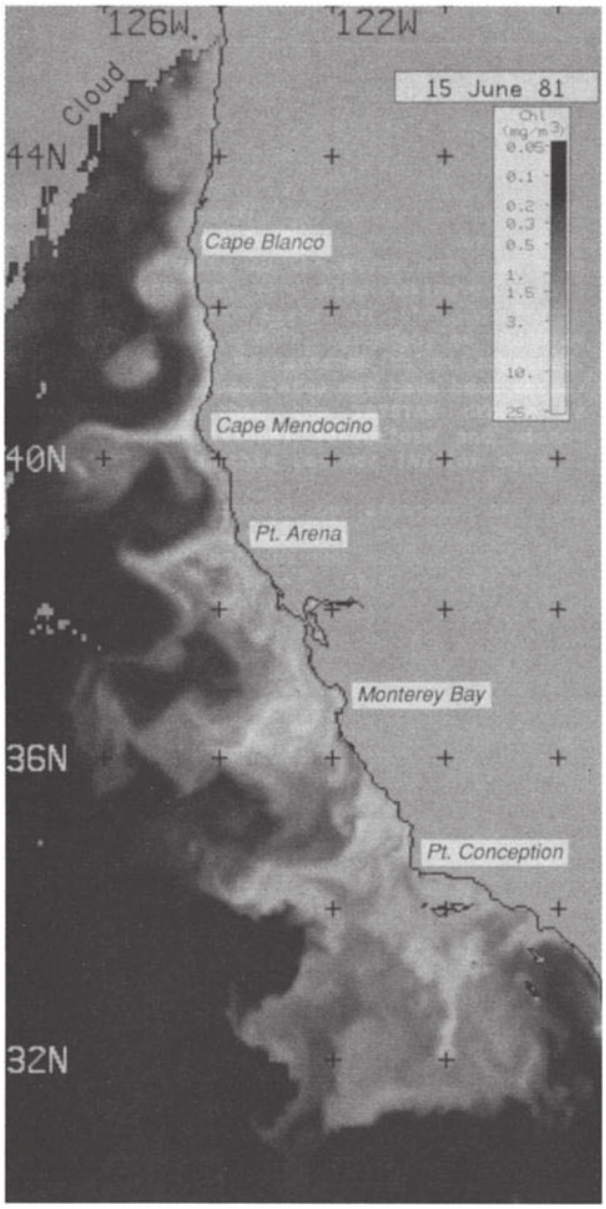

Fig. 17. Surface pigment concentration derived from the CZCS satellite data from June 15, 1981.

To examine the relative magnitudes of offshore and onshore pigment flux, the velocity and pigment concentrations in Figure 8 have been used to calculate the horizontal flux of pigment (the product of normal velocity and pigment concentration) through the upper 100 m of these vertical sections. Although the interpretation of these flux calculations is complicated by the spatially patchy nature of pigment, they provide a more quantitative approach than arguments based simply on the relative positions of pigment and velocity maxima using the same data [*Hood et al.*, 1990; *Chavez et al.*, this issue; *Kosro et al.*, this issue]. The results are that approximately equal amounts of phytoplankton pigment (1.1–1.3 x 10^5 kg day^{-1}) are being transported by the offshore and onshore branches of the meander off Cape Mendocino during the May 18–26 survey (Figure 8*b*). In the meander which appears between stations 9 and 60 in Figure 8*c* during the June 9–18 survey, more pigment (1.3 x 10^5 kg day^{-1}) is being transported in the offshore branch than is returning (0.3 x 10^5 kg day^{-1}) in the onshore branch. This is the meander sampled by the drifter described by *Abbott et al.* [1990]. In both May and June 1987 surveys, approximately 2.5 x 10^5 kg day^{-1} is being transported offshore by the jet at the southwest corner of the surveys. To the extent that the surface drifters in Figure 5 represent the motion of this pigment, most of the biomass and nutrients leaving the survey at its southwest corner remains in meanders and eddies 100–300 km from the coast over the next 10–30 days. During this time, processes such as described by *Abbott et al.* [1990] are likely to transform this pigment into other biological products and detritus, which eventually fall out of the water column. These calculations indicate that at some times the onshore-flowing branch of meanders may carry as much pigment as the offshore-flowing branch, while at other times more is carried offshore than returns. They also indicate that a large amount of biological material is carried offshore to the southwest of Point Arena and Point Reyes, which enriches the ocean in the region 100–400 km from shore.

In some sense, the net biological impact of this system of meanders and eddies can be seen directly in satellite color imagery [*Abbott and Zion*, 1985; *Abbott and Barksdale*, this issue] such as the coastal zone color scanner (CZCS) image from June 15, 1981 in Figure 17, processed as described by *Strub et al.* [1990]. On the basis of the CTZ surveys, we interpret the edge of the region with high pigment concentrations to represent the center of an alongshore jet that flows from north of Cape Blanco to south of Point Arena. There is a detached patch of pigment between capes Blanco and Mendocino, similar to the cold eddy off Cape Blanco in Figure 12, a large meander off Cape Mendocino, similar to Figure 4*b*, which returns near shore north of Point Arena, and an offshore-flowing filament at Point Arena that marks the northern edge of a wider and more convoluted region of high pigment concentrations. At the southern edge of the image, the region of high productivity is interrupted in the Southern California Bight by the "Ensenada Front," where oligotrophic water from the deep ocean flows onshore into the bight [*Peláez and McGowan*, 1986; *Thomas and Strub*,

1990]. Thus although it is likely that processes (squirts and eddies) other than the jet augment productivity inshore of the jet [*Hayward and Mantyla*, 1990; *Chavez et al.*, this issue], the jet is seen to carry nutrients and biomass offshore, along the edge of a region 100–400 km in width, within which the deep ocean is more productive than it is offshore of the jet.

5. Summary and Conclusions

The CTZ and NCCCS surveys in 1987–1988, along with past surveys from the CODE and OPTOMA programs (1981–1986) provide 8 years of evidence with which we can partially answer the questions posed in the introduction. These results apply primarily to the region between approximately 36°N and 42°N during February–July.

5.1. The Spatial Structure of Horizontal and Vertical Transports

5.1.1. *Meandering jet.* Between 39°N and 42°N, the data strongly support the model of a meandering jet, flowing along the offshore border of the region of cold water seen in the satellite images during March–July. We refer to this jet as the seaward jet to distinguish it from other jets that may be present farther inshore. The fact that the jet was closer to the coast in March and stronger than the eddy inshore of the jet [*Magnell et al.*, 1990] suggests a seasonal development that supports the seaward jet as the primary structure in this region and period. The OPTOMA data show the presence of eddies but also support the greater transport in the jet, favoring the meandering jet model. The largest "synoptic" survey in this region, obtained by combining the July 1984 OPTOMA (Figure 14*b*) and CalCOFI data [*Chelton et al.*, 1988], shows a continuous flow from north of Cape Mendocino to south of Point Conception, with eddies inshore and offshore of the jet. Drifters that left the jet in July 1988 and traveled as far west as 134°W did not encounter another southward jet, supporting the contention that the jet which flowed offshore from Point Arena carried most of the surface transport of the California Current at that time and location. We stress that these conclusions apply only to the February–July period; the full seasonal evolution of the system remains to be determined.

A number of features have been found repeatedly, although not universally, in the seaward jet. A tongue of fresh water is often found in the upper 30–50 m of the jet's offshore flank, and a narrow temperature minimum is sometimes found just inshore of the jet's maximum velocity (Figure 8 and 9). This narrow temperature minimum is seen as a cold narrow filament in the satellite images, embedded in the larger region of cool water inshore of the jet. T-S diagrams (Figure 10*b*) show this filament to be nearly isothermal in the upper ocean, resembling the water in the pycnocline beneath the fresh water found just offshore of the maximum velocity, suggesting in situ upwelling within the jet. The mechanism causing this upwelling has yet to be determined, as does its relation to the subsidence described by others. We stress that these conclusions apply to the seaward jet. Other jets and filaments inshore of the seaward jet may have different structures and T-S characteristics.

The presence of the band of fresher water in the upper 20–50 m on the offshore side of the jet at Point Arena supports its continuity with water north of Cape Mendocino and Cape Blanco. The presence of different plankton species offshore, within and inshore of the jet [*Mackas et al.*, this issue; *Hood et al.*, 1990, this issue] also supports the origin of the jet in a water mass farther upstream. The large-scale field of horizontal motion inferred from a sequence of satellite SST images (Figure 12) shows continuity from Cape Blanco to Point Arena during a 3-day period in July 1988, although it also shows that water both leaves and enters the jet along the way, which may contribute to the observed patchiness off Point Arena. The continuous flow from north of Cape Blanco to Point Conception is similar to the path taken by a surface drifter in September–October 1984 [*Thomson and Papadakis*, 1987]. A jet flowing from north of Cape Blanco to south of Cape Mendocino was previously observed in May 1977 by *Freitag and Halpern* [1981]. South of 39°N, the drifters (Figure 7) and satellite-derived field shows that the seaward jet travels through a field of eddies with multiple filaments inshore of the jet, which may be different than the seaward jet and its associated filaments.

5.1.2. *Mesoscale eddy field.* The data show that closed eddies are present in the California Current system. Between 39°N and 42°N, the nearshore hydrography from the March 1987 NCCCS survey and the CTZ surveys show cyclonic eddies located southwest of the capes, inshore of the jet. The eddy surveyed in March is weaker than the jet, as is indicated by the dynamic topography and by the fact that drifters followed the jet but did not become entrained in the eddy [*Magnell et al.*, 1990]. South of 39°N in June–August, the CTZ drifters and hydrography show the presence of both cyclonic and anticyclonic eddies inshore of the jet. Analysis of drifter data by *Brink et al.* [this issue] suggests that eddy and jet transports are roughly equal in this region.

The CTZ and CODE hydrographic data do not extend far enough offshore to determine whether anticyclonic eddies exist offshore of the jet, as has been proposed by others [*Simpson et al.*, 1986; *Mooers and Robinson*, 1984; *Rienecker et al.*, 1987; *Ramp et al.*, this issue]. The OPTOMA data provide most of the hydrographic evidence for the presence of an anticyclonic eddy offshore of the jet between Cape Mendocino and Point Arena, but CTZ drifters in May–June 1987 and June–July 1988, and NCCCS drifters in March of 1987 and 1988 did not map out an eddy in that location. In August 1988, a large anticyclonic eddy offshore of the jet around 35°N was mapped by several CTZ drifters, and a small anticyclonic eddy was found between Cape Mendocino and Point Arena by an NCCCS drifter (although inshore of the cold water boundary), indicating that the drifters are not excluded from mapping such eddies.

Thus the data support the existence of smaller, cyclonic eddies inshore of the jet north of 39°N in March–June and numerous eddies inshore and offshore of the jet south of 39°N in June–August. The long meander that grows off Point Arena in June–July of 1987 and 1988 has a cyclonic eddy within the offshore terminus of the meander, which appears to be cut off and left offshore of the jet in late July 1988, remaining vigorous over at least the next month and moving offshore at approximately 70 km per month (0.03 m s^{-1}), the approximate speed of Rossby wave propagation [*White et al.*, 1990]. Whether these eddies are

present at other times of the year is not known, especially south of 39°N, but the February 1987 cruise, the historical hydrographic data and the altimeter data suggest that eddies between 39°N and 42°N are weaker in winter than summer.

5.1.3. *Squirts.* Most of the evidence does not support the interpretation that the larger filaments in the SST images are squirts, as defined in the introduction. The seaward jet which borders the larger regions of cold water, the band of fresh water found in the outer half of the jet, and the *T-S* characteristics of the narrow cold core of the filaments all argue strongly against a coastal origin of that water. The measurements from current moorings over the shelf north and south of Cape Mendocino show mean southward flow north of the cape and mean northward flow south of the cape during 1987–1988, which has been interpreted as evidence for the nearshore convergence associated with squirts [*Magnell et al.*, 1990]. However, these measurements are also consistent with the confluent flow field created by the meandering jet north of the cape and cyclonic eddy southwest of the cape as determined by the hydrographic data (Figure 3), which provides a more complete picture of the field.

Something looking like a squirt of cold water appears in the sequence of AVHRR images animated to produce the flow depiction shown in Figure 12, emerging between Cape Mendocino and Point Arena over a 3-day period. Whether this is truly a squirt (caused by a nearshore convergence) or cold water pulled from the coast by a pair of previously existing eddies cannot be determined from the images, although its occurrence at the time of a wind relaxation favors the squirt hypothesis. It seems likely that nearshore convergences do produce squirts at times and that they are shorter (100 km) than the long filaments and occur inshore of the observed jet, with time scales of days, contributing to the richness and patchiness of the water properties in that region.

5.2. *Temporal Variability*

Hydrographic data from the CODE, OPTOMA, and CTZ programs between 37°N and 42°N show a seasonal increase in the range of dynamic height fields from winter–spring to summer–fall (Figure 13). This agrees with the interpretation of satellite SST images (Figure 2) and with 1 year of Geosat altimeter data. NCCCS drifters and hydrographic data in March 1987 suggest that the flow field may appear as a jet closer to the coast in early spring, moving farther offshore in April–May. There is some suggestion of a similar behavior in previous analyses of the CODE data, where a southward jet developed initially over the shelf at the time of the spring transition and moved offshore as winds remained upwelling-favorable. This seasonal progression is similar to the wind-driven jet and eddy field modeled by *McCreary et al.* [1991], which suggests that the eddy field could arise from instabilities in a wind-driven jet, making the jet the primary structure.

Hydrographic data and satellite images (Figures 3, 4, 6, and 7) suggest that individual features can grow from a meander 100–150 km from the coast to one 200–225 km from the coast in a period of 2 weeks or less (May 5 to May 18, 1987) and retreat back to the original offshore extent in a similar period (May 18 to June 1, 1987); the jet may leave cutoff eddies in the process (July 16 to July 28, 1988). Features such as the offshore jet at Point Arena may persist for a month in one position (June 20 to July 18, 1988), then reorient in a period of a week or two. Animation of a sequence of satellite images from July 16–18 shows a great deal of structure in currents and SST features with spatial scales of 100 km or less and time scales of several days (Figure 12).

5.3. *Biological Implications*

The jet that flows from north of Cape Mendocino to Point Arena transports nutrient-poor water along its offshore half and nutrient-rich water on its inshore half and appears to separate assemblages of plankton species [*Hood et al.*, 1990, this issue; *Mackas et al.*, this issue]. Although phytoplankton biomass, as represented by phytoplankton pigment concentrations, is generally patchy, it is usually greater inshore and lower offshore of the jet (surface values below 0.5 mg m^{-3} offshore of the jet's center). Moderate pigment concentrations (1–4 mg m^{-3}) may appear in the jet, more often on the inshore or deeper part, where velocities are 0.2–0.5 m s^{-1}. Thus biomass and nutrients are carried along on the inshore half of the jet on its offshore meanders, as is evident in images from the CZCS, which show filaments extending as far offshore as they do in SST images (Figure 17). If meanders create cutoff eddies, the biological material in the eddies remains offshore, as is also evident in CZCS images. Subsidence in the offshore-flowing branch of the meanders may move phytoplankton and nutrients below the euphotic zone and biological processes may transform it during the long meanders. Although the quantitative details of the horizontal and vertical fluxes of nutrients and biomass in these filaments have yet to be determined, the CZCS satellite images suggest that the meandering jet and eddy field creates a region of high productivity that remains mostly inshore of the seaward jet. This region is narrower, on average, north of Point Arena than it is between Point Arena and Point Conception. It is terminated in the Southern California Bight by the onshore advection of oligotrophic water from the deep ocean.

Acknowledgments. The CTZ program was funded by the Coastal Sciences Program of the Office of Naval Research (Code 1122CS). Support for PTS was provided by ONR grants N00014-87K0009 and N00014-90J1115, with additional support provided by NASA grants NAGW-869 and NAGW-1251. Many people contributed to the CTZ data gathering and to the analysis of the data presented here. We especially thank Tim Cowles, John Allen, Steve Pierce, Curt Davis, Burt Jones, Eileen Hofmann, Tim Stanton, Bill Emery, Michele Rienecker, and several anonymous reviewers for their comments. Melinda Stewart and Barbara McVicar helped with the word processing and formatted the final text.

REFERENCES

Abbott, M.R., and B. Barksdale, Phytoplankton pigment patterns and wind forcing off central California, *J. Geophys. Res.*, this issue.

Abbott, M.R., and P.M. Zion, Satellite observations of phytoplankton variability during an upwelling event, *Cont. Shelf Res.*, *4*, 661–680, 1985.

Abbott, M.R., K.H. Brink, C.R. Booth, D. Blasco, L.A. Codispoti, P.P. Niiler, and S.R. Ramp, Observations of phytoplankton and nutrients from a Lagrangian drifter off northern California, *J. Geophys. Res.*, *95*, 9393–9409, 1990.

Allen, J.S., L.J. Walstad, and P.A. Newberger, Dynamics of the coastal transition zone jet, 2, Nonlinear finite amplitude behavior, *J. Geophys. Res.*, this issue.

Batteen, M.L., R.L. Haney, T.A. Tielking, and P.G. Renaud, A numerical study of wind forcing of eddies and jets in the California Current system, *J. Mar. Res.*, *47*, 493–523, 1989.

Bernstein, R.L., L. Breaker, and R. Whritner, California Current eddy formation: Ship, air and satellite results, *Science*, *195*, 353–359, 1977.

Brink, K.H., R.C. Beardsley, P.P. Niiler, M. Abbott, A. Huyer, S. Ramp, T. Stanton, and D. Stuart, Statistical properties of near-surface flow in the California coastal transition zone, *J. Geophys. Res.*, this issue.

Chavez, F., R.T. Barber, A. Huyer, P.M. Kosro, S.R. Ramp, T.P. Stanton, and B. Rojas de Mendiola, Horizontal transport and the distribution of nutrients in the coastal transition zone off northern California: Effects on primary production, phytoplankton, biomass, and species composition, *J. Geophys. Res.*, this issue.

Chelton, D.B., Seasonal variability of alongshore geostrophic velocity off central California, *J. Geophys. Res.*, *89*, 3473–3486, 1984.

Chelton, D.B., A.W. Bratkovich, R.L. Bernstein, and P.M. Kosro, Poleward flow off central California during the spring and summer of 1981 and 1984, *J. Geophys. Res.*, *93*, 10,604–10,620, 1988.

Coastal Transition Zone Group, The Coastal Transition Zone Program, *Eos Trans. AGU*, *69*(27), 697–707, 1988.

Davis, R.E., Drifter observations of coastal surface currents during CODE: The method and descriptive view, *J. Geophys. Res.*, *90*, 4741-4755, 1985.

Dewey, R.K., and J.N. Moum, Enhancement of fronts by vertical mixing, *J. Geophys. Res.*, *95*, 9433–9445, 1990.

Dewey, R.K., J.N. Moum, C.A. Paulson, D.R. Caldwell, and S.D. Pierce, Structure and dynamics of a coastal filament, *J. Geophys. Res.*, this issue.

Emery, W.J., A.C. Thomas, M.J. Collins, W.R. Crawford, and D.L. Mackas, An objective method for computing advective surface velocities from sequential infrared satellite images, *J. Geophys. Res.*, *91*, 12,865-12,878, 1986.

Flament, P., L. Armi, and L. Washburn, The evolving structure of an upwelling element, *J. Geophys. Res.*, *90*, 11,765–11,778, 1985.

Flament, P., P.M. Kosro, and A. Huyer, Mesoscale variability off California as seen by the Geosat altimeter, Proceedings of IGARSS '89, 12th Canadian Symposium on Remote Sensing, *IEEE Publ. 89CH2768-0*, vol. 2, 1063–1068, Inst. of Electr. and Electron. Eng., New York, 1989.

Freitag, H.P., and D. Halpern, Hydrographic observations off northern California during May 1977, *J. Geophys. Res.*, *86*, 4248–4252, 1981.

Haidvogel, D.B., A. Beckmann, and K.S. Hedström, Dynamical simulations of filament formation and evolution in the coastal transition zone, *J. Geophys. Res.*, this issue.

Hayward, T.L., and A.W. Mantyla, Physical, chemical and biological structure of a coastal eddy near Cape Mendocino, *J. Mar. Res.*, *4*, 825–850, 1990.

Hickey, B.M., The California Current system—Hypotheses and facts, *Prog. Oceanogr.*, *8*, 191–279, 1979.

Hood, R.R., M.R. Abbott, A. Huyer, and P.M. Kosro, Surface patterns in temperature, flow, phytoplankton biomass, and species composition in the coastal transition zone of northern California, *J. Geophys. Res.*, *95*, 18,081–18,094. 1990.

Hood, R.R., M.R. Abbott, and A. Huyer, Phytoplankton and photosynthetic light response in the coastal transition zone off northern California in June 1987, *J. Geophys. Res.*, this issue.

Huyer, A.E., Coastal upwelling in the California Current system, *Prog. Oceanogr.*, *12*, 259–284, 1983.

Huyer, A.E., and P.M. Kosro, Mesoscale surveys over the shelf and slope in the upwelling region near Point Arena, California, *J. Geophys. Res.*, *92*, 1655–1682, 1987.

Huyer, A., P.M. Kosro, J. Fleischbein, S.R. Ramp, T. Stanton, L. Washburn, F.P. Chavez, T.J. Cowles, S.D. Pierce, and R.L. Smith, Currents and water masses of the coastal transition zone off northern California, June to August 1988, *J. Geophys. Res.*, this issue.

Ikeda, M., and W.J. Emery, Satellite observations and modeling of meanders in the California Current system off Oregon and northern California, *J. Phys. Oceanogr.*, *14*, 1434–1450, 1984.

Johannessen, J.A., E. Svendsen, S. Sandven, O.M. Johannessen, and K. Lygre, Three-dimensional structure of mesoscale eddies in the Norwegian coastal current, *J. Phys. Oceanogr.*, *19*, 3–19, 1989.

Kadko, D.C., L. Washburn, and B.H. Jones, Evidence of subduction within cold filaments of the northern California coastal transition zone, *J. Geophys. Res.*, this issue.

Kelly, K.A., The influence of winds and topography on the sea surface temperature patterns over the northern California slope, *J. Geophys. Res.*, *90*, 11,783–11,798, 1985.

Kelly, K.A., An inverse model for near-surface velocity from infrared images, *J. Phys. Oceanogr.*, *12*, 1845–1864, 1989.

Kosro, P.M., and A. Huyer, CTD and velocity surveys of seaward jets off northern California, July 1981 and 1982, *J. Geophys. Res.*, *91*, 7680–7690, 1986.

Kosro, P.M., A. Huyer, S. Ramp, R.L. Smith, F. Chavez, T.J. Cowles, M. Abbott, P.T. Strub, R.T. Barber, P.F. Jessen, and L.F. Small, The structure of the transition zone between coastal waters and the open ocean off northern California, spring 1987, *J. Geophys. Res.*, this issue.

Lynn, R.J., and J.J. Simpson, The California Current system: The seasonal variability of its physical characteristics, *J. Geophys. Res.*, *92*, 12,947–12,966, 1987.

McCreary, J.P., Y. Fukamachi, and P.K. Kundu, A numerical investigation of jets and eddies near an eastern ocean boundary, *J. Geophys. Res.*, *96*, 2515–2534, 1991.

Mackas, D.L., K.L. Denman, and A.F. Bennett, Least squares multiple tracer analysis of water mass composition, *J. Geophys. Res.*, *92*, 2907–2918, 1987.

Mackas, D.L., L. Washburn, and S.L. Smith, Zooplankton community patterns associated with a California Current cold filament, *J. Geophys. Res.*, this issue.

Magnell, B.A., J.F. Borchardt, C.L. Greengrove, J.M. Federiuk, and N.A. Bray, Northern California Coastal Circulation Study, data report 2, Main measurement program, March–August 1988, vol. 1, Lagrangian and hydrographic observation, EG&G Washington Anal. Serv. Cent., Inc., Waltham, Mass., 1989*a*.

Magnell, B.A., J.F. Borchardt, C.L. Greengrove, J.M. Federiuk, and N.A. Bray, Northern California Coastal Circulation Study, data report 2, Main measurement program, March–August 1988, vol. 2, Moored instrument, meteorological, and sea level measurements, EG&G Washington Anal. Serv. Cent., Inc., Waltham, Mass., 1989*b*.

Magnell, B.A., N.A. Bray, C.D. Winant, C.L. Greengrove, J. Largier, J.F. Borchardt, R.L. Bernstein, and C.E. Dorman, Convergent shelf flow at Cape Mendocino, *Oceanography*, *3*(1), 4–11, 1990.

Mooers, C.N.K., and A.R. Robinson, Turbulent jets and eddies in the California Current and inferred cross-shore transports, *Science*, *223*, 51–53, 1984.

Moum, J.N., D.R. Caldwell, and P.J. Stabeno, Mixing and intrusions in a rotating cold-core feature off Cape Blanco, Oregon, *J. Phys. Oceanogr.*, *18*, 823–833, 1988.

Narimousa, S., and T. Maxworthy, Application of a laboratory model to the interpretation of satellite and field observations of coastal upwelling, *Dyn. Atmos. Oceans*, *13*, 1–46, 1989.

Paduan, J.D., and P.P. Niiler, A Lagrangian description of motion in northern California coastal transition filaments, *J. Geophys. Res.*, 18,095–18,109, 1990.

Peláez, J., and J.A. McGowan, Phytoplankton pigment patterns in the California Current as determined by satellite, *Limnol. Oceanogr.*, *31*, 927–950, 1986.

Philander, S.G.H., and J.-H. Yoon, Eastern boundary current upwelling, *J. Phys. Oceanogr.*, *12*, 862–879, 1982.

Pierce, S.D., J.S. Allen, and L.J. Walstad, Dynamics of the coastal transition zone jet, 1, Linear stability analysis, *J. Geophys. Res.*, this issue.

Ramp, S.R., P.F. Jessen, K.H. Brink, P.P. Niiler, F.L. Daggett, and J.S. Best, The physical structure of cold filaments near Point Arena, California, during June 1987, *J. Geophys. Res.*, this issue.

Rienecker, M.M., and C.N.K. Mooers, A summary of the OPTOMA program's mesoscale ocean prediction studies in the California Current System, in *Mesoscale/Synoptic Coherent Structures in Geophysical Turbulence*, edited by J.C.J. Nihoul, and B.M. Jamart, pp. 519–548, Elsevier, Amsterdam, 1989*a*.

Rienecker, M.M., and C.N.K. Mooers, Mesoscale eddies, jets, and fronts off Point Arena, California, July 1986, *J. Geophys. Res.*, *94*, 12,555–12,569, 1989*b*.

Rienecker, M.M., C.N.K. Mooers, D.E. Hagan, and A.R. Robinson, A cool anomaly off northern California: An investigation using IR imagery and in situ data, *J. Geophys. Res.*, *90*, 4807–4818, 1985.

Rienecker, M.M., C.N.K. Mooers, and A.R. Robinson, Dynamical interpolation and forecast of the evolution of mesoscale features off northern California, *J. Phys. Oceanogr.*, *17*, 1189–1213, 1987.

Robinson, A.R., J.A. Carton, N. Pinardi, and C.N.K. Mooers, Dynamical forecasting and dynamical interpolation: An experiment in the California Current, *J. Phys. Oceanogr.*, *16*, 1561–1579, 1986.

Schramm, R.E., J. Fleischbein, R. March, A. Huyer, P.M. Kosro, T. Cowles, and N. Dudek, CTD observations in the coastal transition zone off northern California 18–27 May, 1987, *Data Rep. 141, Ref. 88-3*, 191 pp., Coll. of Oceanogr., Oreg. State Univ., Corvallis, 1988.

Send, U., R.C. Beardsley, and C.D. Winant, Relaxation from upwelling in the Coastal Ocean Dynamics Experiment, *J. Geophys. Res.*, *92*, 1683–1699, 1987.

Shannon, L.V., N.M. Walters, and S.A. Mostert, Satellite observations of surface temperature and near surface chlorophyll in the southern Benguela region, in *South African Ocean Color and Upwelling Experiment*, edited by L.V. Shannon, pp. 183–210, Sea Fisheries Research Institute, Cape Town, South Africa, 1985.

Simpson, J.J., T.D. Dickey, and C.J. Koblinsky, An offshore eddy in the California Current system, I, Interior dynamics, *Prog. Oceanogr.*, *13*, 5–49, 1984.

Simpson, J.J., C.J. Koblinsky, J. Peláez, L.R. Haury, and D. Wiesenhahn, Temperature–plant pigment–optical relations in a recurrent offshore mesoscale eddy near Point Conception, California, *J. Geophys. Res.*, *91*, 12,919–12,936, 1986.

Stern, M.E., On the amplification of convergences in coastal currents and the formation of "squirts," *J. Mar. Res.*, *44*, 403–421, 1986.

Strub, P.T., J.S. Allen, A. Huyer, R.L. Smith, and R.C. Beardsley, Seasonal cycles of currents, temperatures, winds, and sea level over the northeast Pacific continental shelf: 35°N to 48°N, *J. Geophys. Res.*, *92*, 1507–1526, 1987*a*.

Strub, P.T., J.S. Allen, A. Huyer, and R.L. Smith, Large-scale structure of the spring transition in the coastal ocean off western North America, *J. Geophys. Res.*, *92*, 1527–1544, 1987*b*.

Strub, P.T., C. James, A.C. Thomas, and M.R. Abbott, Seasonal and nonseasonal variability of satellite-derived surface pigment concentrations in the California Current, *J. Geophys. Res.*, *95*, 11,501–11,530, 1990.

Thomas, A.C., and P.T. Strub, Seasonal and interannual variability of phytoplankton pigment concentrations across a California Current system frontal zone, *J. Geophys. Res.*, *95*, 13,023–13,042, 1990.

Thomson, R.E., and J.E. Papadakis, Upwelling filaments and motion of a satellite-tracked drifter along the west coast of North America, *J. Geophys. Res.*, *92*, 6445–6461, 1987.

Tokmakian, R.T., P.T. Strub, and J. McClean-Padman, Evaluation of the maximum cross-correlation method of estimating sea surface velocities from sequential satellite images, *J. Atmos. Oceanic Technol.*, *7*, 852–865, 1990.

Traganza, E.D., V.M. Silva, D.M. Austin, W.E. Hanson, and S.H. Bronsink, Nutrient mapping and recurrence of coastal upwelling centers by satellite remote sensing: Its implication to primary production and the sediment record, in *Coastal Upwelling: Its Sediment Record*, edited by E. Suess and J. Thiede, pp. 61–83, Plenum, New York, 1983.

Vastano, A.C., and S. Borders, Sea surface motion over an anticyclonic eddy on the Oyashio Front, *Remote Sens. Environ.*, *16*, 87–90, 1984.

Walstad, L.J., J.S. Allen, P.M. Kosro, and A. Huyer, Dynamics of the coastal transition zone in 1987 through data assimilation studies, *J. Geophys. Res.*, this issue.

Washburn, L., D.C. Kadko, B.H. Jones, T.L. Hayward, P.M. Kosro, T.P. Stanton, A. Huyer, S.R. Ramp, and T.J. Cowles, Water mass subduction and the transport of phytoplankton in a coastal upwelling system, *J. Geophys. Res.*, this issue.

White, W.B., C.-K. Tai, and J. DiMento, Annual Rossby waves characteristics in the California Current region from the Geosat exact repeat mission, *J. Phys. Oceanogr.*, *20*, 1297–1310, 1990.

Wyllie, J.G., Geostrophic flow of the California Current at the surface and at 200 m, *CalCOFI Atlas 4*, 12 pp. and 280 charts, State of Calif. Mar. Res. Comm., La Jolla, 1966.

M. R. Abbott, J. A. Barth, R. R. Hood, A. Huyer, C. James, P. M. Kosro, R. L. Smith, P. T. Strub, and L. J. Walstad, College of Oceanography, Oregon State University, Corvallis, OR 97331.

R. T. Barber, Duke University Marine Laboratory, Beaufort, NC 28516.

M. L. Batteen, R. L. Haney, and S. R. Ramp, Naval Postgraduate School, Monterey, CA 93943.

K. H. Brink, Woods Hole, Oceanographic Institution, Woods Hole, MA 02543.

F. P. Chavez, Monterey Bay Aquarium Research Institute, 160 Central Avenue, Pacific Grove, CA 93950.

R. K. Dewey, Science Applications International Corporation, 13400 Northup Way, Suite 36, Bellevue, WA 98005.

D. B. Haidvogel, Institute of Marine and Coastal Sciences, Rutgers University, P.O. Box 231, New Brunswick, NJ 08903.

T. L. Hayward, P. P. Niiler, and M. S. Swenson, Scripps Institution of Oceanography, University of California, San Diego, La Jolla, CA 92093.

D. C. Kadko, Rosenstiel School of Marine and Atmospheric Science, University of Miami, 4600 Rickenbacker Causeway, Miami, FL 33149.

D. L. Mackas, Institute of Ocean Sciences, Sidney, British Columbia, Canada V8L 4B2.

L. Washburn, Department of Geography, University of California, Santa Barbara, CA 93106.

(Received July 16, 1990;
accepted October 26, 1990.)